Network renormalization

Gabrielli, A.; Garlaschelli, D.; Patil, S.P.; Angeles Serrano, M.

nature reviews physics

https://doi.org/10.1038/s42254-025-00817-5

Technical review

Check for updates

Network renormalization

Andrea Gabrielli[1,2,3], Diego Garlaschelli[4,5] ✉, Subodh P. Patil[5] & M. Ángeles Serrano[6,7,8]

Abstract

The renormalization group (RG) is a powerful theoretical framework. It is used on systems with many degrees of freedom to transform the description of their configurations, along with the associated model parameters and coupling constants, across different levels of resolution. The RG also provides a way to identify critical points of phase transitions and study the system's behaviour around them. In traditional physical applications, the RG largely builds on the notions of homogeneity, symmetry, geometry and locality to define metric distances, scale transformations and self-similar coarse-graining schemes. More recently, efforts have been made to extend RG concepts to complex networks. However, in such systems, explicit geometric coordinates do not necessarily exist, different nodes and subgraphs can have different statistical properties, and homogeneous lattice-like symmetries are absent — all features that make it complicated to define consistent renormalization procedures. In this Technical Review, we discuss the main approaches, important advances, and the remaining open challenges for network renormalization.

Sections

[1]Dipartimento di Ingegneria Civile, Informatica e delle Tecnologie Aeronautiche, Università degli Studi 'Roma Tre', Rome, Italy. [2]'Enrico Fermi' Research Center (CREF), Rome, Italy. [3]Istituto dei Sistemi Complessi (ISC) — CNR, Rome, Italy. [4]IMT School for Advanced Studies, Lucca, Italy. [5]Lorentz Institute for Theoretical Physics, University of Leiden, Leiden, The Netherlands. [6]Departament de Física de la Matèria Condensada, Universitat de Barcelona, Barcelona, Spain. [7]Universitat de Barcelona Institute of Complex Systems (UBICS), Barcelona, Spain. [8]ICREA, Barcelona, Spain. ✉e-mail: diego.garlaschelli@imtlucca.it

Key points

- Renormalization group (RG) methods have proven to be indispensable in understanding and classifying the aggregate behaviour of a wide range of physical systems with many degrees of freedom.
- Direct application of RG techniques devised for physical systems is problematic for complex networks, whether due to the absence of intrinsic notions of metric distance, or geometric or topological regularity.
- In spite of these challenges, notable progress has been made in a number of restricted settings, which we survey in this Technical Review.
- Numerous open questions remain, and we summarize the case for a more broadly applicable network renormalization programme grounded on first principles, which we attempt to articulate.

Introduction

Renormalization and renormalizability are notions that underpin the modern physical understanding of material phenomena in the Universe. They posit that at large enough spatiotemporal scales, small-scale details average out, and explain why we do not need to know the precise behaviour of subatomic particles to navigate daily life. Formalizing renormalization, however, took physicists several decades, and lead to spectacular insights into the universality of certain physical phenomena. Box 1 summarizes the basic notions of renormalization and renormalization group (RG) transformations as traditionally applied to physical systems.

Beyond 'traditional' physics systems, large complex systems in nature and society also contain multiple interacting scales, with no prior preferred resolution level. Can renormalizability also be applied in such cases? For instance, when modelling the flow of goods and services between businesses, can their relationships be consistently represented when aggregating firms into broader categories, such as economic sectors? Likewise, when considering epidemic spread on a network, one is interested in understanding whether long-term aggregate outcomes differ from compartment-based analyses, factoring in modelling and parameter uncertainties.

Although it may be tempting to transpose lessons from the study of physical systems wholesale to complex networks, several key assumptions must be critically re-examined. These include the locality of interactions and the underlying spatial regularity typical in materials, where disorder is treated as a small perturbation. Furthermore, upon considering dynamical processes on networks, it is essential to ensure that any coarse-graining approach is consistent with the dynamics, both for specific realizations and for the statistical ensembles they derive from. Thus, it is necessary to revisit the foundational premise of renormalization — the idea of averaging over small scales to understand aggregate behaviour — and reformulate it in the specific context of complex networks.

In this Technical Review, we explore the application of renormalization techniques to complex networks. We discuss how real-world networks, often lacking explicit geometric embeddings, and featuring heterogeneity and intertwined connectivity across multiple scales require a rethinking of the renormalization programme. We review existing methods that implement network renormalization based on a variety of coarse-graining prescriptions. We then examine approaches that aim to generalize the core tenets of RG to account for network heterogeneity and disorder from different premises, and conclude by highlighting open problems and questions yet to be addressed in this developing field.

Challenges for renormalization of complex networks

RG methods have shown that large classes of systems exhibit universal features, proving valuable for building bottom-up models of natural phenomena. However, in real-world applications, interactions rarely exhibit the homogeneity modelled by regular lattices. Instead, structural disorder and spatially inhomogeneous interactions give rise to network patterns with topological and geometrical heterogeneity. Real-world networks are characterized by a broad distribution of the number of links per node (degree), a short average path length (the small-world property) even in large networks, a non-vanishing local triangle density (finite clustering) even in sparse networks, and a modular (possibly hierarchical) community structure, among other properties[1–4]. These irregularities challenge the extension of standard RG approaches. The challenges are compounded by difficulties arising from the finiteness of the systems one seeks to represent, requiring explicit accounting of boundary and finite-size effects[5–9].

RG analysis, as commonly implemented, is defined by three fundamental steps:

- **Definition of coarse-grained variables** either in real space, by tiling the latter with identical mesoscopic cells or 'blocks' containing multiple microscopic units, or in dual k-space, by decomposing such variables in different wavelength components, from the shortest to the longest;
- **Averaging out, or marginalizing over the finer details** of the system, represented by local fluctuations, that is, the properties of either the small-scale cells or the short-wavelength (fast) modes;
- **Renormalization of the couplings and parameters** of the system whose interactions have been coarse-grained. (In theories with a continuum of degrees of freedom, renormalization also necessitates a prescription to deal with the infinities that inevitably arise. This prescription is well understood in the context of particle physics and statistical field theory[10,11], but will not be needed in the present context given the discrete and finite nature of complex networks).

These operations can be iterated, generating an RG flow whose trajectories and fixed points can be studied.

The first step — defining the coarse-grained variables — is in principle straightforward for homogeneous physical systems with local interactions embedded in translationally invariant metric spaces (such as regular lattices or Euclidean geometries), given that notions of distance and neighbourhood make 'identical mesosocopic cells' or 'wavelength' straightforward to define (for example, a 2D lattice can be readily coarse-grained onto a reduced lattice with the same symmetry and dimensionality). In systems with all-to-all homogeneous interactions, as idealized in mean-field models, the structure can also trivially be mapped onto another all-to-all graph. However, defining coarse-grained variables becomes non-trivial in highly inhomogeneous and small-world networks, posing the question: how can one appropriately define block nodes or slow modes in this context? Moreover, such networks are often constructed using empirically informed resolution levels, typically constrained by data limitations. For instance, epidemic spread

and economic shocks are often observed at aggregate levels (such as subpopulation contacts or economic sector flows) rather than at finer scales where the actual dynamics takes place (individual infections or firm-level propagating shocks). Modelling processes directly at these aggregate levels often fails to capture the dynamics of the system at finer scales, as shown in studies of shock transmission during the 2008 financial crisis and epidemic spread during the Covid-19 outbreak[12,13].

Similarly, in homogeneous lattices or metric spaces, the second step — averaging out local fluctuations — leverages internal symmetries to replace notions of connectedness with proximity defined via coordinatization, where spatially closer nodes are more likely to connect. Physical theories on such spaces are local, and coarse-grained theories only involve local fields and their finite-order derivatives. However, notions of locality do not straightforwardly extend to irregular networked spaces. In symmetric binary networks, alternatives include defining interactions via the adjacency matrix (nearest-neighbour) or its powers (up to n^{th}-neighbour interactions), or using a discrete metric induced by the minimum path length[14]. The sparsity of networks, the heterogeneous distribution of the number of neighbours at different path distances, and the presence of disordered long-range interactions — key to the small-world property — complicate unambiguous definitions of locality in complex networks.

Finally, the complexities in the third step — renormalizing couplings and parameters — are closely linked to those in the preceding steps. In disordered lattice systems such as spin glasses[15], interaction topologies may be regular but coupling constants may be very heterogeneous. This heterogeneity can be modelled using random variables, where self-averaging ensures that spatial averages correspond to distributional averages. In such situation, renormalizing couplings entails mapping the probability distribution of fine-scale coupling constants onto an induced distribution for coarse-grained constants[16]. In heterogeneous networks, the challenge is amplified, as the interaction topology itself is disordered. Many complex network models correspond to random graphs drawn from some ensemble with specified properties. Consequently, renormalizing couplings and parameters requires mapping an initial probability distribution over fine-grained graphs to a new distribution over coarse-grained graphs. In principle, this mapping defines a renormalization flow, with its own functional trajectories and fixed points.

Motivated by these considerations, in recent years, researchers have aimed to establish a general framework for the renormalization of complex networks. In what follows, we aim to summarize a selection of methods that use different yet related strategies towards this goal. We first provide a broad (but inevitably non-exhaustive) overview of approaches to coarse-grain complex networks, after which we delve into specific methods that extend one or more of the three steps of the renormalization programme outlined above in the context of heterogeneous networks.

Network coarse-graining approaches

The absence of underlying lattice structures for most real-world complex networks complicates the identification of consistent coarse-graining schemes and has inspired a variety of approaches that can be classed into several broad categories.

Box 1 | Renormalization in statistical physics and field theory

In physical systems, locality and causality of interactions conspire to limit the influence of small-scale fluctuations so that only a handful of parameters describe the system at macroscopic scales. Steps towards formalizing this idea were made in the 1960s, when Leo Kadanoff applied the concept of coarse-graining (studied earlier by Paul and Tatiana Ehrenfest[167]) to statistical mechanical systems in order to understand their behaviour in the neighbourhood of a critical point of a second-order phase transition[118].

One such system is the Ising model, in which lattice spins undergo a phase transition between disordered and ordered (or magnetized) phases. The model is amenable to being coarse-grained by introducing 'block-spin' degrees of freedom. The scaling of interactions between the block-spin variables as one coarse-grains was formalized through the renormalization group (RG)[111]. Early numerical calculations on a lattice[168] were followed by more general variational methods[169–172].

The RG marked a breakthrough in statistical mechanics by providing a real-space method to formally average over small-scale system details, thereby defining effective degrees of freedom and interactions at any given scale, which became the foundation for RG methods in continuum field theories, developed further by Kenneth Wilson some years later[113,173]. Wilson's work not only provided a theoretical basis for understanding scaling behaviour in critical phenomena, but also formalized what had previously been a piecemeal approach to addressing nominally divergent quantities in field theories. These divergences stem from the mathematical idealization of resolving arbitrarily small distances, for which a subtraction scheme had been proposed[174]. However, this scheme lacked a firm conceptual foundation until the RG was developed. Since then, RG methods have enabled the development of a 'theory of theories', which reveals how disparate physical systems with vastly different microscopic details can exhibit universal behaviour near their critical points[175–179].

Over the past five decades, the adoption of RG techniques spread to encompass diverse domains, ranging from cosmology at the largest scales to particle physics at the smallest. In the wider context of statistical mechanics, RG methods have been extended to out-of-equilibrium systems on homogeneous and fractal lattices[180–186], where calculations are facilitated by local and translation-invariant interactions. Important examples extending beyond the initial applications include models of epidemic dynamics[187], biological swarms[188–190], neural networks[191–194], dynamical and directed percolation[195,196], voter models for opinion dynamics[197], and synchronization models of nonlinear oscillators, such as the Kuramoto model[120,121] on 1D chains[198], lattices[199] and hierarchical trees[200]. Furthermore, RG methods have found fruitful application in systems abstracted as tensor networks[192,201–203], or in frameworks defined by their information-theoretic content[204–208].

In contrast to equilibrium settings, the relevant ingredients that determine universality classes in non-equilibrium systems are sometimes unknown, and, in general, no RG calculation is available at higher orders in perturbative treatments. Non-perturbative RG has emerged as a promising alternative[209–212] and, for example, has been applied to the diffusive epidemic model in lattices[213].

Methods based on shortest paths

An important attempt to network coarse-graining uses the length of shortest paths to define node distance, enabling an iterative RG transformation based on box-covering methods developed for fractal geometries[17,18]. This approach groups nodes within a given shortest path distance to form coarse-grained nodes at a larger resolution, thereby generating an RG sequence[14]. The method has unveiled self-similar and fractal features[14,19–21], suggested new growth mechanisms[22] and led to a classification of networks into universality classes[5,23]. However, owing to the small-world property, RG transformations that use shortest paths as a metric criteria turn out to be inadequate for disentangling and uncovering scaling behaviour. Consequently, self-similarity of the degree distribution under these transformations is not accompanied by the scaling of correlations, particularly for clustering.

In addition, real-space RG transformations have been proposed based on the addition of long-range links to an underlying regular lattice with short-range connectivity. Such transformations have been used to investigate problems such as the behaviour of the Watts–Strogatz model near its critical point (in the limit where the density of shortcuts tends to zero[24]) and of a scale-free network model on lattices whose original topological properties remain unchanged after transformation[25]. However, these methods require prior knowledge of the node coordinates, or equivalently of the distinction between short-range links (defining the only path lengths actually involved in the coarse-graining) and long-range ones. This information is often not known or sometimes even defined for real-world networks.

Spectral methods

An alternative approach is based on the spectral properties of networks. These methods coarse-grain nodes in a manner that preserves the behaviour of a specific process. The spectral coarse-graining method, originally devised for random walks on networks, ensures the preservation of large-scale behaviour by maintaining the largest eigenvalues of the stochastic matrix and the corresponding eigenvectors, effectively decimating fast modes while leaving the slow modes unchanged[26]. This method has been extended to bipartite networks[27] and applied to synchronization dynamics of coupled oscillators, where the network Laplacian becomes the relevant operator[28–30]. Similar spectral coarse-graining ideas have been used in the study of synchronization in directed networks[31] and controllability[32]. The possibility of developing a field-theoretic RG approach to order–disorder phenomena using eigenvectors and eigenvalues of the graph Laplacian[33] was further explored using deterministic hierarchical networks, such as the Cayley tree and the diamond lattice for the Gaussian model[33,34]. These approaches pave the way for a more comprehensive notion of graph renormalization based on Laplacian spectra[35], to which we devote a separate section later in this Technical Review.

Topological methods

Parallel to the aforementioned approaches, coarse-graining procedures based on topological properties have been also proposed. Some of these techniques rely on node centrality measures such as the degree[36] or generalized degree[37]; node similarity measures based on neighbour overlap[38], including traditional notions of structurally equivalent nodes in social networks[39] and trophically equivalent species in food webs[40]; and network motifs as recurrent patterns[41].

Decimation schemes such as degree-thresholding renormalization[42] and the k-core decomposition[43] warrant special mention. The former removes nodes with a degree below a certain threshold to define a hierarchy of nested subgraphs; the latter was specifically designed to decompose a network into a sequence of maximal subgraphs, in which every vertex has a certain minimum degree. These methods have proven effective in real systems in revealing hierarchical self-similarity beyond the scale invariance of the degree distribution, such as the scaling of the clustering spectrum.

Additionally, strategies based on modularity in the context of multiscale community detection[44] have been proposed, analogous to multilevel graph partitioning algorithms in computer science. Such algorithms encompass coarsening heuristics based on nodes or edge properties, such as the heavy-edge heuristic for graphs with uniform distributions of connections, which merges nodes linked with large weights[45]. For graphs with power-law degree distribution, there are community-based coarsening schemes that collapse groups of highly interconnected vertices[46].

Topological methods are based on the existence of specific structural patterns, such as (hierarchical) community structure or structurally equivalent nodes, and fail in their absence. This limitation is at odds with typical implementations of renormalization in physics, where one would like to consistently and iteratively coarse-grain a system as simple as a lattice even in the absence of mesoscopic features.

Symmetry-based methods

Another approach uses equivalence classes defined via process-based symmetries to define a coarse-graining prescription. In contexts from biology to computer science, local symmetries that characterize the processes on a network provide a general principle for defining the building blocks of a system[47]. In particular, networks for which node transformations leave the so-called input trees invariant give rise to emergent equitable partitions[48], which has been used to define concepts such as the lumpability of ordinary differential equations[49,50], Boolean backward equivalence[51] and fibration colouring[52].

The utility of these methods is evidenced by the fact that symmetry-induced equitable partitions make it possible to reduce to a set of dynamical variables that preserves the overall dynamics and synchronization[53]. Although extremely useful as network reduction techniques that identify process-based equivalence classes of nodes, symmetry-based approaches typically identify a single partition (usually corresponding to the maximal network reduction). As with purely topological approaches, they cannot be iterated and do not generalize to contexts where symmetries are absent.

Coarse-graining in engineering and computer science

Methods to develop scaled-down engineering models of the internet, along with other communication and transportation networks, have been a recurrent objective in the field of communication technologies[54–56]. More recently, reducing the size of a graph without substantially altering its relevant properties has also become an important topic in machine learning, where graph embeddings and deep learning techniques such as graph neural networks are increasingly applied to graph-structured data. Coarse-graining schemes look to compress graphs to reduce computational cost and complexity for practical applications[57–63], and are useful in designing efficient error-correcting codes for communication and data storage. An RG approach has been used to generate small network codes that enable efficient computation of belief propagation performance in tree-like networks[64]. Although these methods are driven by network renormalization ideas, they are typically focused on specific processes, providing limited insight into the fundamental principles governing the multiscale nature of graph-structured data and complex systems.

Information-theoretic approaches

Information-theoretic methods have been developed to explore the interplay between scales on networks. The phenomenon of causal emergence[65], in which a higher scale provides a more informative description of the network's connectivity, leads to minimization of the uncertainty in observations of relationships between nodes. Additionally, for dynamics on a particular graph, multiple coarse-grained descriptions capturing different features of the original process may exist. Information-theoretic measures can aid in assessing how partitioning the state space of a dynamical process on a network influences the projected dynamics[66].

Towards principled renormalization approaches

The heterogeneity of real-world networks can make some approaches inconsistent with each other, and this inequivalence calls for a broader first-principles based framework for the renormalization of complex networks. Constructing such a framework necessitates revisiting the roots of the renormalization programme that is now relatively well understood for systems defined on regular lattices and homogeneous metric spaces, while being mindful of the challenges discussed in the previous section. In what follows, we review various attempts to address these challenges through different approaches. To facilitate the discussion, we first lay some common ground to orient the reader.

We first address the definition of coarse-grained variables. To fix notation, it is convenient to introduce the $N_\ell \times N_\ell$ adjacency matrix $A^{(\ell)}$ representing the network at a given scale of resolution — that is, a given hierarchical level (or layer) ℓ — where N_ℓ is the number of nodes observed at that level. The case $\ell = 0$ may denote the 'finest-grained' level (that is, the native level at which network data are available), whereas $\ell > 0$ denotes the ℓth level of iteration of the coarse-graining process (when considering fine-graining approaches, we will also admit 'negative levels' $\ell < 0$, as explained further). For weighted networks, one is also interested in the weight matrix $W^{(\ell)}$ representing the strength of links.

The coarse-graining of the variables can be implemented in different ways. Approaches that generalize the 'real-space' renormalization procedure focus on defining coarse-grained variables in terms of 'block nodes' that determine the rows and columns of the adjacency matrix at the next level. For these approaches, the equivalent of 'defining a spatial tiling' is the definition of a certain partition Ω_ℓ mapping the N_ℓ nodes $\{i_\ell\}_{i_\ell=1}^{N_\ell}$ observed at level ℓ onto a smaller set of $N_{\ell+1}$ coarser nodes (or 'blocks') $\{i_{\ell+1}\}_{i_{\ell+1}=1}^{N_{\ell+1}}$ at the next level $\ell+1$. Approaches that try to generalize the k-space renormalization procedure focus instead on defining an extended notion of 'dual space' for arbitrary graphs, possibly via an explicit operator representation of the adjacency matrix that decomposes the latter into fundamental modes.

Regarding integrating out the fine details in real space, doing so means defining a surjective (many to one, and therefore not invertible in general) mapping from $A^{(\ell)}$ onto $A^{(\ell+1)}$ (and from $W^{(\ell)}$ onto $W^{(\ell+1)}$ if applicable), whereas in k-space it entails defining a similar mapping between successive instances of the dual operator. A natural choice is that of assuming a local mapping, that is, one where the entry $A^{(\ell+1)}_{i_{\ell+1}j_{\ell+1}}$ of the coarse-grained matrix is chosen to depend only on the entries $\{A^{(\ell)}_{i_\ell j_\ell}\}_{i_\ell \in i_{\ell+1}, j_\ell \in j_{\ell+1}}$ of the fine-grained matrix that involve the microscopic nodes contained in $i_{\ell+1}$ and $j_{\ell+1}$, that is,

$$A^{(\ell+1)}_{i_{\ell+1}j_{\ell+1}} = \mathcal{F}\left(\{A^{(\ell)}_{i_\ell j_\ell}\}_{i_\ell \in i_{\ell+1}, j_\ell \in j_{\ell+1}}\right) \tag{1}$$

where $\mathcal{F}$ denotes a certain function. As a useful example, it should be noted that at a purely binary level, a link from block $i_{\ell+1}$ to block $j_{\ell+1}$ is present if and only if at level ℓ, there is at least one link from any node 'inside' $i_{\ell+1}$ (that we denote as $i_\ell \in i_{\ell+1}$) to any node 'inside' $j_{\ell+1}$ (similarly denoted as $j_\ell \in j_{\ell+1}$). This coarse-graining step produces the adjacency matrix $A^{(\ell+1)}$ with the following entries:

$$A^{(\ell+1)}_{i_{\ell+1}j_{\ell+1}} = 1 - \prod_{i_\ell \in i_{\ell+1}} \prod_{j_\ell \in j_{\ell+1}} (1 - A^{(\ell)}_{i_\ell j_\ell}). \tag{2}$$

Similarly, one can introduce a local scheme to obtain the coarse-grained matrix $W^{(\ell+1)}$ from $W^{(\ell)}$:

$$W^{(\ell+1)}_{i_{\ell+1}j_{\ell+1}} = \mathcal{G}\left(\{W^{(\ell)}_{i_\ell j_\ell}\}_{i_\ell \in i_{\ell+1}, j_\ell \in j_{\ell+1}}\right), \tag{3}$$

where $\mathcal{G}$ denotes a function. Note that the freedom of choosing $\mathcal{F}$ and $\mathcal{G}$ leads to scheme dependence, which is a generic caveat in any RG implementation. Importantly, as noted above, $\mathcal{F}$ and $\mathcal{G}$ are surjective and therefore not invertible in general: these properties correspond to the desired loss of small-scale information, making the RG a semigroup. The same property applies to dual-space approaches via the lossy integration of fast modes.

Finally, one needs to generalize the renormalization of couplings and model parameters. If the network is a single deterministic graph (an empirical network, for example) supporting a specific interaction model or process, then this step depends on the nature and parameters of the interaction itself. In certain cases where the process is in one-to-one correspondence with the procedure used to represent the network in dual space, this step can follow directly from integrating out the fine details, as discussed in detail for the case of a diffusion process in the section on Laplacian network renormalization. In contrast, if the 'network' is not deterministic and is instead represented as a random graph model (with its own parameters) with multiple statistical draws already at the original resolution $\ell = 0$, then renormalizing the couplings also entails renormalization of the random graph parameters, as discussed in the sections on geometric network renormalization and multiscale network renormalization. Doing so necessitates a separate analysis of the functional flow of induced probability distributions over graphs and random graph model parameters. Importantly, at its fixed point (where the probability distribution no longer changes its shape, but only its parameters) the RG flow might be statistically 'inverted', that is, one might reverse the flow of the probability distribution from higher levels to lower ones, only through a parameter change. If applied at the native level $\ell = 0$, this inverse flow might actually produce fine-grained ($\ell < 0$) versions of the network, with a larger number of nodes and, in general, a sparser topology.

Armed with these clarifications, we proceed to present three different approaches that address the three steps as discussed in the introduction in complementary ways.

Geometric network renormalization

Spatial locality in complex networks can be restored within a geometric framework[67], in which the structural heterogeneity and non-locality of real-world networks is rendered local through embedding in hyperbolic spaces, restoring the applicability of a geometric RG[68–71].

Geometric model

The geometric soft configuration model[42,72] imposes metric distances between nodes based on popularity and similarity dimensions. These

dimensions are abstract and their combination results in hyperbolic geometry emerging as a natural space that can embed hierarchical and small-world organization. The distances in this space encode the likelihood that two nodes will form a connection, with closer nodes more likely to connect. This is similar to the approach used in random geometric graphs[73,74] and latent space models for social networks[75].

In the Newtonian version of the model, known as the $\mathbb{S}^D$ model[42], each node i_0 (with $i_0 = 1,\ldots,N_0$) at level $\ell = 0$ is assigned a popularity variable and coordinates in a similarity space. Popularity is encoded by a hidden degree κ_{i_0} drawn from some arbitrary distribution, $\rho(\kappa)$, typically a power law with exponent $-\gamma$ ($\gamma > 0$). In dimension $D = 1$, the similarity space is a 1D sphere with radius R_0, chosen to accommodate N_0 nodes with constant density in which each node i_0 is assigned an angular coordinate θ_{i_0} defining angular distances $\Delta\theta_{i_0 j_0}$ between pairs of nodes i_0, j_0. The probability $p_{i_0 j_0}$ that nodes i_0 and j_0 are connected takes a gravity-law form[76] and defines a maximum-entropy[2] ensemble

$$p_{i_0 j_0} = \frac{1}{1+\chi_{i_0 j_0}} \tag{4}$$

where

$$\chi_{i_0 j_0} = \frac{(R_0 \Delta\theta_{i_0 j_0})^{\beta}}{(\mu_0 \kappa_{i_0} \kappa_{j_0})^{\max(1,\beta)}}. \tag{5}$$

The parameter μ_0 sets the average degree $\langle k \rangle_0$, and the individual expected degrees are proportional to the κ values of the corresponding nodes. β controls clustering in the topology of the network, reflecting the triangle inequality in the latent space, and acts as an inverse temperature[76,77].

The model exhibits an anomalous topological phase transition at $\beta = 1$ (ref. 77). In the geometric phase, corresponding to $\beta > 1$, clustering is finite[42], whereas it vanishes in the thermodynamic limit of the non-geometric phase, $0 \leq \beta \leq 1$. However, in the quasi-geometric regime $0.5 \lesssim \beta < 1$, clustering decays to zero very slowly[78], implying that finite networks still retain a substantial level of clustering, comparable to that of some real-world complex networks. Thus, lower temperatures imply mostly short-range links, whereas higher temperatures balance the likelihood of different link lengths.

The $\mathbb{S}^D$-model has a purely geometric formulation, the $\mathbb{H}^{D+1}$ model[72], in which the hidden degree κ is mapped to a radial coordinate r, which converts the connection probability (equation (4)) into a Fermi–Dirac function depending solely on the distances between nodes in hyperbolic space. The Mercator tool[79,80] uses statistical inference and machine learning techniques to embed real networks in this space by maximizing the congruence between the observed network structure and the $\mathbb{S}^D$ (equivalently, $\mathbb{H}^{D+1}$) model[81]. The maps can then be used for various downstream tasks, such as visualization, analysis, navigation and renormalization.

This family of models is highly effective in explaining key features of the connectivity of real networks, such as heterogeneous degree distributions[42,72,82], significant clustering[42,72,82–84], small-world phenomena[42,85–87], percolation characteristics[88–90], spectral aspects[91] and self-similarity[42]. The framework has also been expanded to explain preferential attachment in growing networks[92], weighted networks[93], bipartite networks[94,95], networks driven by complementarity[96], multilayer networks[97,98], networks with community structures[99–101], directed networks[102] and networks where nodes have associated features[103].

Geometric renormalization technique

The $\mathbb{S}^1$ or $\mathbb{H}^2$ model establishes a foundation for a geometric renormalization (GR) group for complex networks by acting iteratively on the hyperbolic map of a network[68–71]. Upon assigning coordinates in the embedding space at level $\ell = 0$, a new layer $\ell = 1$ is obtained through coarse-graining and rescaling. This involves partitioning the similarity subspace into N_1 sectors — the first of the three renormalization steps — via a partition Ω_0 whereby nodes $\{i_0\} \in i_1$ within the same sector i_1 (with $i_1 = 1,\ldots,N_1$) become supernodes. The supernodes are linked if there is at least one connection between their original nodes as in equation (2) (Fig. 1a), thereby averaging out the finer details. Upon iteration, this process generates a renormalization flow across scales $\ell \geq 0$ by progressively selecting longer-range connections.

GR reveals multiscale self-similarity as a ubiquitous symmetry in real-world networks across domains[68,71], and accurately predicts the self-similarity observed in multiscale reconstructions of human brain connectomes, indicating their proximity to the critical structural transition between the small-world and non-small-world regimes[104] (Fig. 1b). These findings are explained by the renormalizability of the $\mathbb{S}^1$ or $\mathbb{H}^2$ model in the geometric ($\beta > 1$)[68] and non-geometric ($\beta \leq 1$)[71] regimes. The scale transformation for the hidden degrees is obtained by imposing that the connection probability (equation (4)) remains invariant. The flow of the angular coordinate can be defined by any transformation that preserves the rotational invariance of the original model. Using the notation $z_{i_\ell} = \kappa_{i_\ell}^{\max(1,\beta)}$, the transformations that preserves the probability of connection and, consequently, the topological features of the network in the renormalization flow, are

$$z_{i_{\ell+1}} = \sum_{i_\ell \in i_{\ell+1}} z_{i_\ell}, \quad \theta_{i_{\ell+1}} = \frac{\sum_{i_\ell \in i_{\ell+1}} z_{i_\ell} \theta_{i_\ell}}{\sum_{i_\ell \in i_{\ell+1}} z_{i_\ell}}. \tag{6}$$

with our usual convention of $i_\ell \in i_{\ell+1}$ denoting nodes that belong to the supernode $i_{\ell+1}$. The above transformations renormalize the couplings and parameters.

The global parameters evolve as $R_{\ell+1} = R_\ell / r^\ell$, $\mu_{\ell+1} = \mu_\ell / r^{\min(1,\beta)}$, where r is the number of nodes in equally sized supernodes and β is scale invariant. These transformations satisfy the semigroup property: renormalizing twice with groups of r nodes equals renormalizing once with groups of r^2. The probability $p_{i_{\ell+1} j_{\ell+1}}$ retains the original form of $p_{i_\ell j_\ell}$, and the average degree $\langle k \rangle$ is a relevant observable with a flow $\langle k \rangle_{\ell+1} = r^\nu \langle k \rangle_\ell$ when $\beta > 1$ (ref. 68). This behaviour also applies to real networks as long as they admit a good embedding. A value $\nu > 0$, typical of real networks, indicates a flow towards a highly connected graph; if $\nu < 0$, the network flows towards a 1D ring; at the transition between the small-world and non-small-world phases, $\nu = 0$ and the average degree stays preserved (see the Supplementary Information for more details). Finally, for $\beta \leq 1$, the number of links remains constant under renormalization[71].

Extension to weighted networks

The weighted structure of a network is retained in the RG flow by imposing a transformation of weights that preserves the relationship between weights and degree. In this way, the geometric renormalization of weights (GRW) technique[70] produces the multiscale unfolding of a weighted network structure[105,106] into a shell of self-similar layers. GRW is sustained by the renormalizability of the weighted $\mathrm{W}\mathbb{S}^D$ ($\mathrm{W}\mathbb{S}^D$) model[93]. In practice, an effective approximation with practical advantages is to select the maximum weight of the renormalized links.

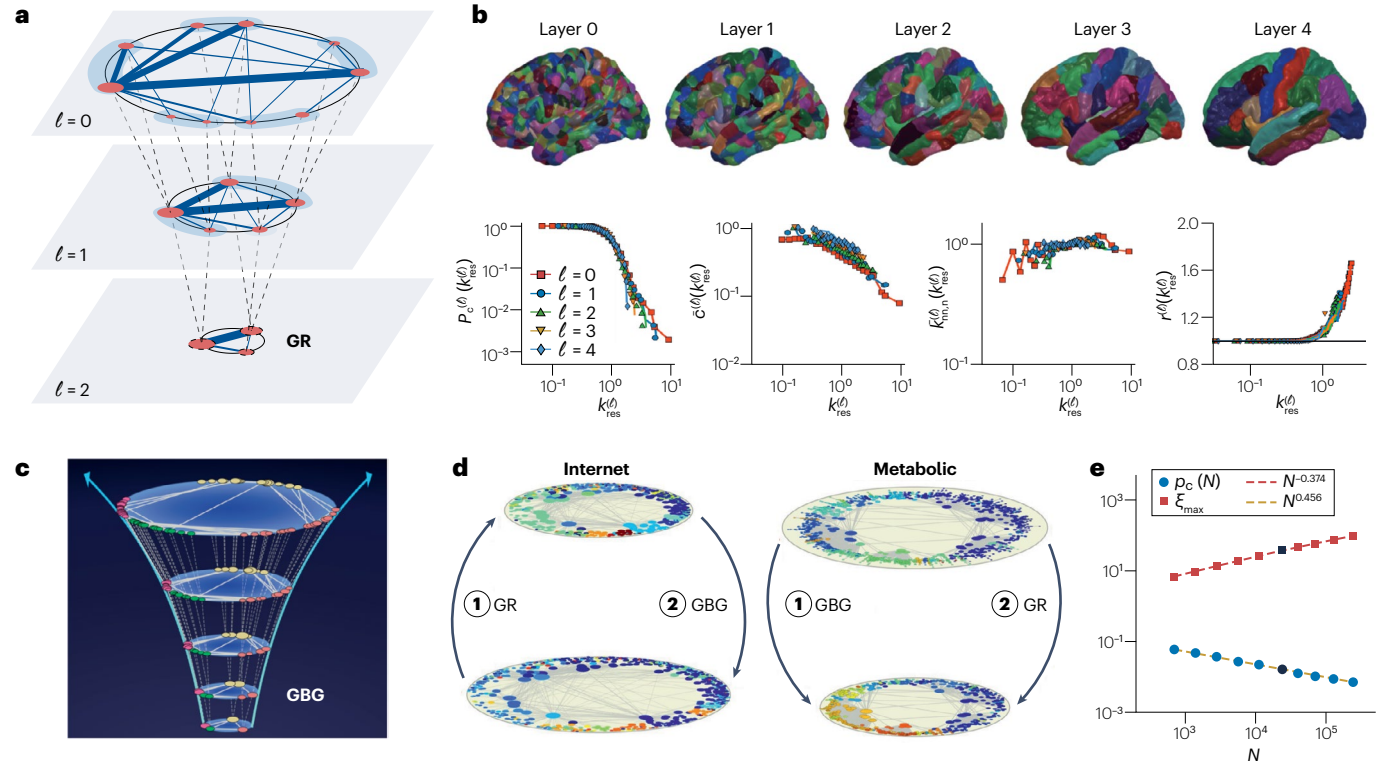

Fig. 1 | Direct and inverse methods and results for geometric network renormalization on real networks. a, Sketch of the geometric renormalization (GR) transformation. In layer $\ell = 0$, non-overlapping blocks of $r = 2$ consecutive nodes shaded in blue are defined along the similarity circle, thereby inducing a partition Ω_0 of the original N_0 nodes into $N_1 = N_0/r$ blocks. The blocks are coarse-grained and represented as supernodes in layer $\ell = 1$. Each supernode is assigned an angular coordinate within the region defined by the constituent nodes in $\ell = 0$. Finally, two supernodes in $\ell = 1$ are connected as described in equation (2). The process can be iterated to produce layer $\ell = 2$ from $\ell = 1$. Owing to the semigroup property, layer $\ell = 2$ can also be produced directly from $\ell = 0$ by forming blocks of size $r = 4$ nodes. **b**, GR replicates the multiscale connectivity structure of human brain connectomes. Multiscale hierarchical representations are reconstructed at five length scales from anatomical data (top row). The topological properties (bottom) of the connectomes at each scale ℓ (symbols) are well reproduced by GR applied to the geometric map of the largest-resolution layer (lines). From left to right, these properties are the complementary cumulative degree distribution $P_c(k_{res})$, the clustering coefficient $\bar{c}(k_{res})$, the normalized average degree of nearest neighbours $\bar{k}_{nn,n}(k_{res}) = \bar{k}_{nn}(k_{res})\langle k\rangle/\langle k^2\rangle$, and the rich-club coefficient $r(k_{res})$. These quantities were calculated as a function of the rescaled degree $k_{res} = k/\langle k\rangle$ to account for the variation of the average degree across layers. **c**, The geometric branching growth process (GBG) evolves networks in a self-similar fashion. **d**, GBG is a statistical inverse of GR, such that the GBG transformation, when applied to a renormalized layer of the internet, recovers a statistical equivalent to the original internet network. Likewise, applying GR to a GBG-grown surrogate of the human metabolic network recovers the original architecture. **e**, The combination of GR and GBG offers a way to study critical phenomena using finite-size scaling in single-instance real networks, providing a method to estimate the corresponding critical exponents numerically. To illustrate this, results of a bond percolation process mimicking random links failures in the internet are shown as a function of the network size, N_ℓ. The critical bond occupation probability, p_c, and the maximum, ξ_{max}, of the susceptibility are well fitted by power laws. The black symbols indicate the original network. The GBG and GR shells were produced with branching rate $b = 2$ and block size $r = 2$. These results suggest a vanishing percolation threshold in the internet graph, as expected in scale-free networks. Part **a** adapted from ref. 70, Springer Nature Limited. Part **b** reprinted with permission from ref. 104, PNAS. Parts **c** and **d** adapted with permission from ref. 69, PNAS. Part **e** reprinted with permission from ref. 69, PNAS.

Weighted networks with heterogeneous degree distributions, from very different domains — including metabolic networks in the cell, flights among commercial airports, scientific collaboration networks, and more — show geometric scaling when coarse-grained and rescaled using this strategy, named sup-GRW, or the theoretically based transformation[70] (see the Supplementary Information for details).

Self-similar fine-graining

A technique that reverses GR is the geometric branching growth (GBG) model[69]. This model accurately predicts the self-similar behaviour of real-world growing networks, such as the World Trade Web and the journal citation network over long time spans. It operates by generating self-similar metric expansions that replicate the original structure of the network, up to arbitrarily large network size.

To produce a GBG fine-grained layer $\ell - 1$ starting from layer ℓ ('backwards' with respect to the coarse-graining direction) nodes in the original layer are divided into r descendants with a probability p (Fig. 1c), so that the population increases as $N_{\ell-1} = N_\ell(1 + p(r-1)) = bN_\ell$ with branching rate b. Nodes that do not split retain their coordinates, and each descendant node is assigned new coordinates. The hidden degrees of the descendants must adhere to GR by satisfying equation (6), and their distribution, $\rho(z)$, must preserve that of the ancestor layer and, consequently, must be a stable distribution[107]. Additionally, their angular coordinates are fixed with a slight angular offset to the

left and right of their ancestors, preserving their rotational ordering. Further details are given in the Supplementary Information. Once coordinates are assigned to descendants, connections in the new layer are implemented to ensure the resulting network belongs to the $\mathbb{S}^1$ ensemble.

Iterative application of GBG, with $\mu_{\ell-1} = b\mu_\ell$, produces a sequence of progressively fine-grained self-similar layers, meaning that the original empirical connection probability, degree distribution, clustering coefficient and community structure are preserved in the flow, whereas the average degree decreases. An inflationary version of GBG, with extra links added with $\mu_{\ell-1} = a\mu_{\ell-1}$ and $a > 1$, avoids the average degree decreasing very fast or increases it. GBG is a statistical inverse of GR (Fig. 1d), and inflationary GBG is a statistical inverse of deflationary GR, where pruning links decreases the average degree. The renormalization of both the weighted and unweighted $\mathbb{S}^1$ model accurately replicate the multiscale self-similarity observed in real networks, suggesting that the same principles determine network connectivity at different scales for both long-range and short-range connections over time.

Applications

In combination, GR and GBG provide a top-to-bottom multiscale unfolding of a network across all scales. Applications include the design of multiscale methods, such as multiscale navigation[68], which improve the performance of single-scale protocols. Scaled-down and scaled-up replicas of real networks[68,69] that preserve their statistical properties including the density of connections, are readily derived from geometric renormalization techniques. These replicas allow investigation of size-dependent phenomena in real networks, an extremely useful prospect for applications such as the study of size-induced stochastic resonance effects, exploring critical behaviour by applying finite-size scaling techniques[69] (Fig. 1e), and enabling model reduction for high-fidelity simulation of otherwise computationally expensive processes.

Laplacian network renormalization

Another general approach for the renormalization of complex networks[35,108] uses the concept of Laplacian diffusion between nodes[109,110] to induce a run-time detection of multiscale structures, thereby coarse-graining the vertices and edges of a generic network, and ultimately renormalizing dynamical models defined on the network. Like the geometric approach described in the previous section, this framework can be formulated in an intuitive and physically illustrative real-space version, strongly analogous to the Migdal–Kadanoff RG approach in statistical physics[111,112]. However, its distinctive character is its rigorous formulation in terms of a dual, or k-space representation, in the spirit of Wilsonian RG[113]. In both cases, this framework introduces an iterative prescription for coarsening networks while preserving their diffusion dynamical features at progressively larger spatiotemporal scales.

Laplacian diffusion as neighbourhood detector

The first step in formulating the Laplacian renormalization group (LRG) approach for heterogeneous undirected (binary or weighted) networks lies in defining 'equivalent' neighbourhoods of different nodes at any fixed scale, by using the symmetric graph Laplacian operator[110,114] $L^{(0)}$, constructed at the initial hierarchical level $\ell = 0$ from the adjacency matrix $A^{(0)}$ and having entries $L^{(0)}_{i_0 j_0} = k_{i_0}\delta_{i_0 j_0} - A^{(0)}_{i_0 j_0}$, where $\delta_{i_0 j_0}$ is the Kronecker delta symbol and $k_{i_0} = \sum_{j_0=1}^{N_0} A^{(0)}_{i_0 j_0}$ is the degree of node i_0 (with $i_0 = 1,\ldots,N_0$).

If $\mathbf{X}^{(0)}(\tau)$ is any diffusive field defined on the network at time τ (with $X^{(0)}_{i_0}(\tau)$ the node-i_0 component of the field) and governed by the heat diffusion equation $\dot{\mathbf{X}}^{(0)}(\tau) = -L^{(0)}\mathbf{X}^{(0)}(\tau)$, one can formally write

$$\mathbf{X}^{(0)}(\tau) = K^{(0)}(\tau)\mathbf{X}^{(0)}(0) = \mathrm{e}^{-\tau L^{(0)}}\mathbf{X}^{(0)}(0), \tag{7}$$

where $K^{(0)}(\tau) \equiv \mathrm{e}^{-\tau L^{(0)}}$ is the diffusion evolution operator. The element $K^{(0)}_{i_0 j_0}(\tau)$ gives the fraction of field diffused from node j_0 to i_0 (and vice versa) in a time τ through all possible paths connecting the two nodes[115,116].

Denoting the eigenvalues of $L^{(0)}$ as $\{\lambda^{(0)}_i\}_{i=1}^{N_0}$ (with $\lambda^{(0)}_1 \le \lambda^{(0)}_2 \le \cdots \le \lambda^{(0)}_{N_0}$) and the corresponding eigenvectors as $\{\boldsymbol{\lambda}^{(0)}_i\}_{i=1}^{N_0}$, and focusing on connected undirected networks, all eigenvalues satisfy $\lambda^{(0)}_i \ge 0$ with only one null eigenvalue, and the eigenvectors can be chosen to be orthogonal. $K^{(0)}(\tau)$ shares the same eigenvectors with corresponding eigenvalues $0 < \mathrm{e}^{-\lambda^{(0)}_i \tau} \le 1$. Note that τ can be viewed as a scale measure on the network: a larger τ corresponds to a larger neighbourhood of nodes connected by diffusion. For instance, in a lattice, at each τ there is a corresponding identical spatial scale $l = \sqrt{D\tau}$, where D is the diffusion constant. In this sense $K^{(0)}(\tau)$ induces an optimal partition of the network at each τ (ref. 117).

Real-space Laplacian renormalization group

Thanks to its physical interpretation, one can use $K^{(0)}(\tau)$ to partition the N_0 nodes of the original ($\ell = 0$) network at each arbitrary τ into N_1 'diffusionally equivalent' subgraphs, which can then be coarse-grained into macronodes (also known as supernodes) to define the network at the next hierarchical level ($\ell = 1$). One can then adopt a decimation recipe to set the new renormalized edges between supernodes starting from the connections at the microscopic scale, as in equations (1) and (3). In regular lattices, because fixing τ is equivalent to fixing the spatial scale l, this procedure leads to coarse-graining in exactly the style of the Kadanoff method of generating block spins for the Ising model[118].

Laplacian coarse-graining for networks can be summarized as follows. First, define the binarized Laplacian matrix $\zeta^{(0)}(\tau)$ with entries

$$\begin{cases} \zeta^{(0)}_{i_0 j_0}(\tau) = 1 & \text{if } K^{(0)}_{i_0 j_0}(\tau) \ge \min[K^{(0)}_{i_0 i_0}(\tau), K^{(0)}_{j_0 j_0}(\tau)] \\ \zeta^{(0)}_{i_0 j_0}(\tau) = 0 & \text{otherwise} \end{cases} \tag{8}$$

Note that $\zeta^{(0)}(\tau = 0)$ is the $N_0 \times N_0$ identity matrix and $\zeta^{(0)}_{i_0 j_0}(\tau \to \infty) = 1$ for all i_0, j_0. At a fixed $\tau^* > 0$, the matrix $\zeta^{(0)}(\tau^*)$ can be seen as the adjacency matrix of a metagraph of the original network, comprising N_1 different connected components diffusionally connected at the scale τ^*. This procedure induces a partition Ω_0 of the original N_0 nodes into $N_1 < N_0$ supernodes (Fig. 2a). The larger τ^* is, the fewer and bigger such connected components. For $\tau^* \to \infty$ there is only a single cluster, because all network nodes are finally connected by the uniform diffusion field. The coarse-grained weighted adjacency matrix $W^{(1)}$, along the lines of equation (3), can be simply defined by weighted macroedges between all pairs of supernodes with a weight equal to the appropriately normalized sum of the micro-edges connecting the two corresponding clusters at the finer scale (Fig. 2b). Alternatively, one can adopt any consistent decimation procedure, in analogy with coarse-graining in statistical physics, to obtain a binary adjacency matrix $A^{(1)}$ (for instance, by equation (1)). The entire process can be iterated to define all higher hierarchical levels $\ell > 1$ (Fig. 2c,d).

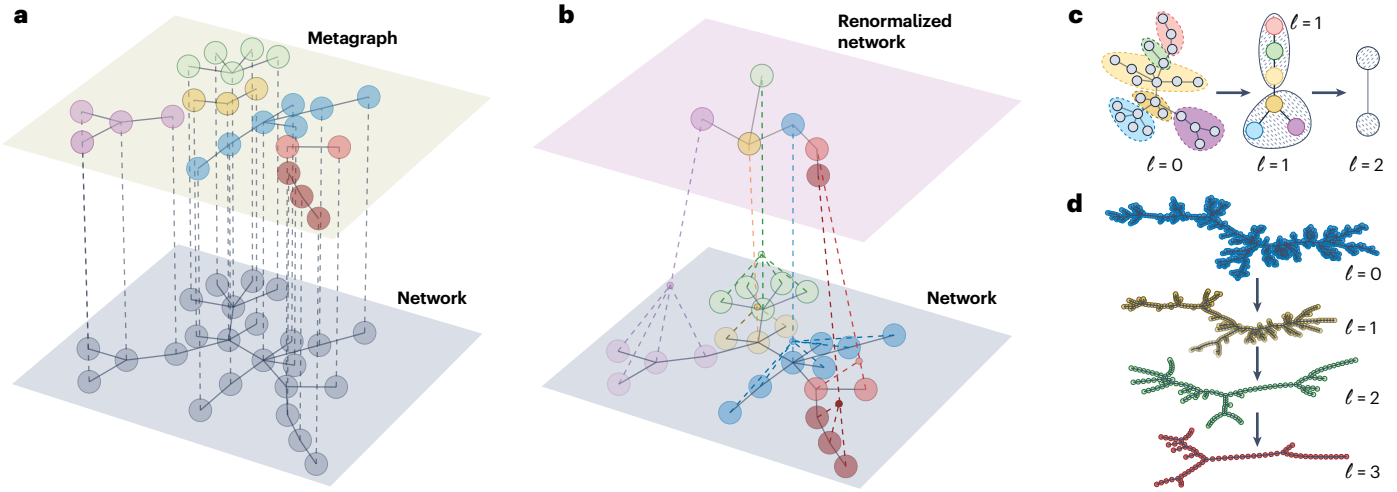

Fig. 2 | Real-space construction in the Laplacian network renormalization approach. a, The lower layer ($\ell = 0$) represents the original network $A^{(0)}$, here a Barabási–Albert network (evolved by adding one node with $m = 1$ links at a time, until a final size of $N_0 = 24$ nodes is reached), and the upper layer illustrates the partition Ω_0 obtained for a diffusion timescale $\tau^* = 1.96$. Different colours identify the N_1 Kadanoff supernodes. **b**, Following Ω_0, each block is lumped into a single supernode i_1 (with $i_1 = 1,\ldots,N_1$) incident to any edge to the original ones, to create the coarse-grained network $A^{(1)}$ at the next hierarchical level $\ell = 1$. **c**, Three steps of the real-space Laplacian renormalization group (LRG) process. **d**, LRG coarse-graining of a random tree. Figure reprinted from ref. 108, CC BY 4.0.

k-space formulation of the LRG

This formulation proceeds in direct analogy with Wilson's RG approach in continuum field theories[119], and explicitly manifests the semigroup property. It can be seen as a Fourier-space counterpart of the real-space LRG, with the Fourier basis given by the Laplacian eigenvectors with wave-modes replaced by the Laplacian eigenvalues. On regular lattices these eigenvectors indeed coincide with the usual plane-wave Fourier basis with eigenvalues given simply by k^2.

This approach offers a deeper insight into the renormalization process and permits not only to coarse-grain the network, but also to appropriately rescale statistical-dynamical models (such as Ising or contact processes) embedded in it in order to detect and study characteristic (correlation) scales and possible phase transitions. Because $L^{(0)}$ and $K^{(0)}(\tau)$ are Hermitian, we adopt the quantum 'bra–ket' formalism to write

$$L^{(0)} = \sum_{i=1}^{N_0} \lambda_i^{(0)} |\lambda_i^{(0)}\rangle\langle\lambda_i^{(0)}|.$$

The completeness of the eigenvectors ensures the meaningful definition of coarse-grained variables. The subsequent steps are implemented by the following renormalization procedure in the manner of Wilson[35]:

- Fix a time τ^* that sets the new resolution scale (or lower cut-off).
- Partition the Laplacian spectrum into two sets: $n(\tau^*)$ 'fast' eigenvalues $\lambda_i^{(0)} \geq \lambda^* \equiv 1/\tau^*$, and $N_0 - n(\tau^*)$ 'slow' eigenvalues $\lambda_i^{(0)} < \lambda^*$.
- Integrate out the 'fast' ($\lambda_i^{(0)} \geq \lambda^*$) region of the spectrum and redefine the 'truncated' Laplacian that retains the contribution of the $N_0 - n(\tau^*)$ slow eigenvectors with $\lambda_i^{(0)} < \lambda^*$: $L_{\mathrm{red}}^{(0)}(\tau^*) = \sum_{i=1}^{N_0 - n(\tau^*)} \lambda_i^{(0)} |\lambda_i^{(0)}\rangle\langle\lambda_i^{(0)}|$. This procedure corresponds to the second step of the RG programme.
- Rescale the time, $\tau' = \tau/\tau^*$, so that τ^* becomes the new time unit, implying a renormalization of the coarse-grained Laplacian to the hierarchical level $\ell = 1$ as $L^{(1)} \equiv \tau^* L_{\mathrm{red}}^{(0)}(\tau^*)$. This is the third RG step.

Iterating these steps produces the renormalized Laplacian $L^{(\ell)}$ at generic levels $\ell > 1$ of aggregation. This *k*-space formulation of LRG can be complemented by a real-space interpretation (see Supplementary Information).

The statistical field formulations of the Ising model, contact processes and most statistical models characterized by local translational invariant interactions on regular lattices all admit a Gaussian approximation whose kernel is completely determined by the Laplacian operator, which is diagonal in the Laplacian plane-wave basis on lattices[120,121]. This remains true for the same models on irregular networks[34,122,123], the only difference being that the Laplacian operator is no longer translationally invariant. Such a Gaussian approximation is the only exactly solvable field theory in all cases, with non-Gaussian interactions usually considered through perturbation approaches around it. This is one of the key points of Wilson's RG: the Fourier basis is the one in which the exactly solvable Gaussian approximation is diagonal, that is, determined by a superposition of independent orthogonal variables. Rescaling is performed in this basis to take advantage of the straightforward reparametrization of the Gaussian approximation, while studying the details of the transformation of the non-Gaussian terms. LRG generalizes this approach to irregular networks, seen as non-local and heterogeneous embedding spaces for the statistical models.

Finally, the spectral dimension of Laplacians on network simplicial complexes has also been explored[124,125] and generalizations of the LRG scheme to networks constructed from simplicial complexes and higher-order interactions have also been proposed[126,127] (see the Supplementary Information).

Statistical physics interpretation of the diffusion evolution operator

The operator $K^{(0)}(\tau)$ can be used to build an 'intrinsic scales scanner' for networks. The 'scanner' possesses all the mathematical properties of the entropic susceptibility or heat capacity for equilibrium

statistical physics, so that pronounced maxima (diverging in the infinite size limit) of this quantity indicate a sort of phase transitions in the network structural organization. Indeed, the eigenvalues $\{e^{-\lambda_i^{(0)}\tau}\}_{i=1}^{N_0}$ of $K^{(0)}(\tau)$ can be used to define the run-time probability density function $\rho(\lambda;\tau)=\sum_{i=1}^{N_0}\delta(\lambda-\lambda_i^{(0)})e^{-\lambda\tau}/Z(\tau)$ where $Z(\tau)=\sum_{i=1}^{N_0}e^{-\lambda_i^{(0)}\tau}$, where $\delta(\lambda)$ is the usual Dirac delta function. This measure has an associated Shannon entropy $S(\tau)=-\sum_{i=1}^{N_0}\rho(\lambda_i^{(0)};\tau)\log[\rho(\lambda_i^{(0)};\tau)]$. Because $L^{(0)}$ for undirected networks is Hermitian and positive semidefinite, $S(\tau)$ can be formally seen also as the von Neumann entropy $S[\rho(\tau)]=-\mathrm{Tr}[\rho(\tau)\log\rho(\tau)]$, related to the quantum canonical density operator $\rho(\tau)=K^{(0)}(\tau)/\mathrm{Tr}[K^{(0)}(\tau)]$ (refs. 109,128,129), where $L^{(0)}$ plays the role of the Hamiltonian and τ that of the inverse temperature[130,131]. Equivalently, one can say that $Z(\tau)=\mathrm{Tr}[K^{(0)}(\tau)]$ is the partition function related to the free energy $F(\tau)$ by $F(\tau)=-\tau^{-1}\log Z(\tau)$.

A direct consequence of this formal analogy is that the quantity

$$C(\tau)=-\frac{\mathrm{d}S(\tau)}{\mathrm{d}\log\tau} \tag{9}$$

has the mathematical properties of an entropic susceptibility — that is, a heat capacity[35,129]. A singularity of $C(\tau)$ at a certain scale τ^* in the limit of an infinite number of nodes, or a pronounced peak in the finite but large N case, can be interpreted as a phase-transition point. In other words, τ^* is an intrinsic network scale at which the topology of the network changes abruptly, like what happens at the correlation length scale in the Ising model. For instance, in a stochastic block model[132] with densely connected blocks of the same size and weaker interblock connections, $C(\tau)$ has two peaks, one at the diffusion scale of the single blocks and another at the larger scale of the interblock typical paths. In this sense, $C(\tau)$ works as a detector of intrinsic scales, which can guide the coarse-graining procedure of a network by singling out the characteristic scales at which the network structure shows topological transitions[117].

Topologically scale-invariant networks

A network is topologically scale invariant if $\omega(\lambda)\sim\lambda^{\gamma}$, where $\omega(\lambda)$ is the Laplacian eigenvalue density, with $\gamma=d_s/2-1$ and d_s being the Laplacian spectral dimension[133] (see the Supplementary Information). In this case, the entropic susceptibility is independent of τ and has the constant value $C(\tau)=d_s/2$ (ref. 35). This independence of τ is seen in regular lattices or random trees, but also in more complex networks such as hierarchical modular networks[134]. Owing to the definition of the LRG as discussed in this section, all topologically scale-invariant networks keep the same topology under Laplacian scale transformations and coarse-graining[135] (see also ref. 136). Thus, $C(\tau)$ can be used as a detector of scale invariance on real networks, and if it has a constant value then it gives a direct measure of the spectral dimension.

Multiscale network renormalization

The multiscale network renormalization approach[137–139] aims to introduce a random graph model that is consistent under arbitrary node aggregation. Its motivation originates from two (related) considerations. On the one hand, for a given network, different node partitions may be relevant for different reasons (for instance, because the different methods discussed in this Technical Review might indicate different coarse-grainings of nodes): one should therefore be ready to model the same system consistently under different possible node aggregations. On the other hand, in real-world network data, the meaning of 'nodes' is not always homogeneous: sometimes, although the majority of nodes represents the system's units observed at a certain hierarchical level (individual firms in a production network, for example), other nodes might represent aggregations at coarser hierarchical levels (entire sectors, or even countries, each one aggregating several firms). Both considerations imply that a unique random graph model of the system under consideration should be applicable coherently (that is, it should produce consistent probability distributions of graphs) after having aggregated (or disaggregated) nodes arbitrarily.

This requirement means that the multiscale renormalization approach aims at remaining completely agnostic with respect to the definition of coarse-grained variables: one may 'tile' the set of nodes arbitrarily, that is, introduce any desired partition Ω_0, without relying on any notion of metric or diffusional proximity. Regarding averaging out fine details, in principle the approach allows for different choices but, concretely, the choice in equation (2) is made[137] in light of applications where any connection between constituent nodes (such as individual firms) is relevant for defining connections between supernodes (such as countries or economic sectors). In any case, the distinctive aspect of the multiscale approach is the identification of a fixed point of the RG flow where an exact renormalization of couplings and parameters can be carried out for arbitrary node aggregation, as we explain in this section.

Invariance under node aggregation

The sought-for notion of aggregation-invariant random graphs is similar in spirit to the concept of stable random variables[140–142] — that is, random variables that remain distributed according to the same law after being combined together (for instance, after taking their sum[141,142] or their maximum[143,144]). Here, using the notation introduced at the end of the section on coarse-graining approaches, one considers a random graph ensemble that produces a specific realization $A^{(\ell)}$ of the graph with probability $P_\ell(A^{(\ell)}|\mathbf{\Theta}_\ell)$, where $\mathbf{\Theta}_\ell$ is the set of all parameters of the model. Given the probability distribution $P_\ell(A^{(\ell)}|\mathbf{\Theta}_\ell)$ and an arbitrary partition Ω_ℓ, a resulting graph ensemble is also induced at the next level $\ell+1$, described by a certain probability distribution $P_{\ell+1}(A^{(\ell+1)}|\mathbf{\Theta}_{\ell+1})$ (Fig. 3a). The key idea of the multiscale renormalization approach[137] is the identification of a functional form of the graph probability that remains invariant across all hierarchical levels, for all possible partitions (as a result, one can drop the subscript ℓ from P_ℓ). Only the (renormalized) parameters $\mathbf{\Theta}_{\ell+1}$ are allowed to depend on the level $\ell+1$, and in general are related to $\mathbf{\Theta}_\ell$ through Ω_ℓ. This condition corresponds to the exact renormalization of parameters via the identification of the fixed point of the RG flow in the space of graph probabilities.

Multiscale model with independent edges

It is possible to find the explicit fixed-point $P(A^{(\ell)}|\mathbf{\Theta}_\ell)$ in the case of graph models with independent edges. For such models, $P(A^{(\ell)}|\mathbf{\Theta}_\ell)$ factorizes in terms of the connection probabilities $p_{i_\ell j_\ell}(\mathbf{\Theta}_\ell)$ between pairs of nodes $i_\ell j_\ell$ as

$$P(A^{(\ell)}|\mathbf{\Theta}_\ell)=\prod_{i_\ell j_\ell}[p_{i_\ell j_\ell}(\mathbf{\Theta}_\ell)]^{A^{(\ell)}_{i_\ell j_\ell}}[1-p_{i_\ell j_\ell}(\mathbf{\Theta}_\ell)]^{1-A^{(\ell)}_{i_\ell j_\ell}}. \tag{10}$$

The multiscale model (MSM)[137] is defined as the unique non-trivial fixed point of the RG flow in the space of connection probabilities — that is, the one fulfilling the scale-invariant requirement under the choice in equation (2), which is

$$p_{i_\ell j_\ell}(\mathbf{\Theta}_\ell)=\begin{cases}1-e^{-\delta x_{i_\ell}x_{j_\ell}f(d_{i_\ell j_\ell})}, & i_\ell\neq j_\ell\\ 1-e^{-\delta x_{i_\ell}^2 f(d_{i_\ell i_\ell})/2}, & i_\ell=j_\ell\end{cases} \tag{11}$$

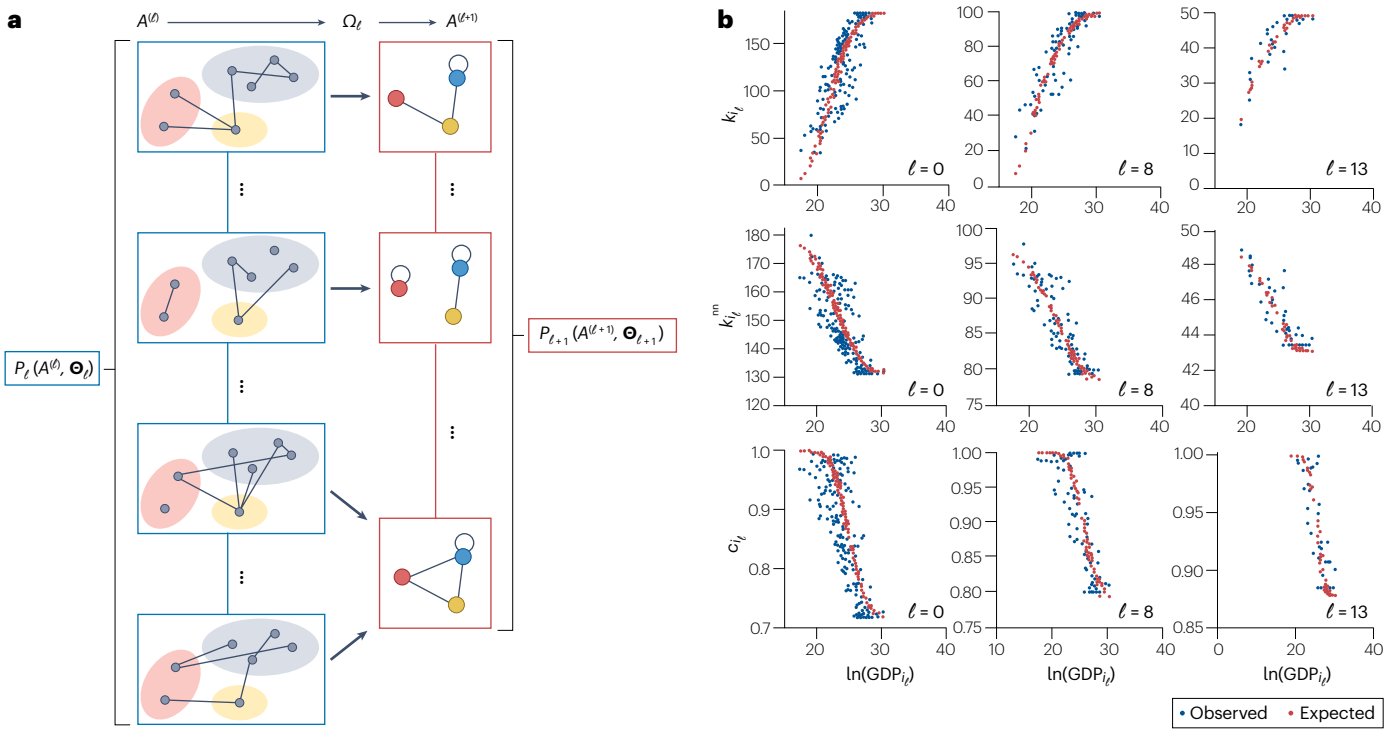

Fig. 3 | The multiscale network renormalization approach. a, Given a probability distribution $P_\ell(A^{(\ell)}|\mathbf{\Theta}_\ell)$ of graphs with adjacency matrix $A^{(\ell)}$ and set of all parameters $\mathbf{\Theta}_\ell$, a node partition Ω_ℓ is used to map sets of nodes onto 'block nodes' of the resulting coarse-grained graphs with adjacency matrix $A^{(\ell+1)}$. A link from $i_{\ell+1}$ to $j_{\ell+1}$ is drawn if a link from i_ℓ to j_ℓ is present, for any $i_\ell \in i_{\ell+1}, j_\ell \in j_{\ell+1}$. Note that multiple graphs at level ℓ may end up in the same graph at level $\ell+1$. This coarse-graining therefore induces a new probability distribution $P_{\ell+1}(A^{(\ell+1)}|\mathbf{\Theta}_{\ell+1})$ over graphs at the next level. The multiscale approach looks for the scale-invariant form of this probability. **b**, Prediction of local topological properties of the renormalized international trade network across various levels of geographical aggregation, using the multiscale model. Top row, observed and expected degree k_{i_ℓ} versus $\ln(\mathrm{GDP}_{i_\ell})$ for all N_ℓ nodes, for three representative hierarchical levels ℓ_1, ℓ_2, ℓ_3 such that $N_{\ell_1} = 183$ (left), $N_{\ell_2} = 100$ (centre) and $N_{\ell_3} = 50$ (right). Middle row, observed and expected average nearest-neighbour degree $k^{nn}_{i_\ell}$ versus $\ln(\mathrm{GDP}_{i_\ell})$ for all N_ℓ nodes, for the same three hierarchical levels. Bottom row, observed and expected local clustering coefficient c_{i_ℓ} versus $\ln(\mathrm{GDP}_{i_\ell})$ for all N_ℓ nodes, for the same three hierarchical levels. GDP, gross domestic product. Figure reprinted from ref. 137, CC BY 4.0.

where the parameters $\mathbf{\Theta}_\ell$ have been decomposed into one global parameter $\delta > 0$ that tunes the overall density of links in the network, a set of N_ℓ positive node-specific additive parameters $\{x_{i_\ell}\}_{i_\ell=1}^{N_\ell}$ (called 'fitness' values) that determine the different individual tendencies of nodes of establishing connections, and (optionally) a set of N_ℓ^2 dyadic parameters $\{d_{i_\ell j_\ell}\}_{i_\ell, j_\ell=1}^{N_\ell}$ representing node-pair effects such as node-to-node similarity, distance or membership of common communities. The function f is an arbitrary monotonic and positive-valued function.

Parameter renormalization and aggregation invariance

When the partition Ω_ℓ is used to coarse-grain the network to the next level $\ell+1$, the probability of a configuration $A^{(\ell+1)}$ is still described exactly by equations (10) and (11), with ℓ replaced by $\ell+1$ and with parameters renormalized as[137]

$$x_{i_{\ell+1}} = \sum_{i_\ell \in i_{\ell+1}} x_{i_\ell}, \quad d_{i_{\ell+1} j_{\ell+1}} = f^{-1}\left(\frac{\sum_{i_\ell \in i_{\ell+1}} \sum_{j_\ell \in j_{\ell+1}} x_{i_\ell} x_{j_\ell} f(d_{i_\ell j_\ell})}{\sum_{i_\ell \in i_{\ell+1}} \sum_{j_\ell \in j_{\ell+1}} x_{i_\ell} x_{j_\ell}}\right), \quad (12)$$

whereas δ is scale invariant, that is, it remains unchanged under renormalization.

In the special case when $\{d_{i_\ell j_\ell}\}_{i_\ell, j_\ell=1}^{N_\ell}$ are ultrametric (that is, $d_{i_\ell j_\ell}$ can be represented as the distance of nodes i_ℓ and j_ℓ to their common branching point in a dendrogram where nodes are the leaves), they also become unchanged under renormalization, that is, $d_{i_{\ell+1} j_{\ell+1}} = f^{-1}\left(f(d_{i_\ell j_\ell})\right) = d_{i_\ell j_\ell}$ for any $i_\ell \in i_{\ell+1}$ and $j_\ell \in j_{\ell+1}$ (ref. 137). In another special case, all dyadic effects can be switched off by setting $f(d) \equiv 1$, so that the model is entirely fitness driven. Crucially, the fitness parameters themselves cannot be switched off and represent the irreducible features to be considered in the model.

Notably, it is possible to calculate the exact partition function $Z(\delta)$ corresponding to equation (11) and show that it takes the same value irrespective of the level ℓ at which it is calculated[137], confirming that the MSM sits at a fixed point of the renormalization flow (see the Supplementary Information). Unlike the geometric or Laplacian approaches discussed in previous sections, the MSM requires neither an embedding metric space with node coordinates, nor a notion of diffusional proximity, in order to guide the renormalization procedure. Indeed, every partition is allowed by the model, which therefore shows a more general aggregation invariance with respect to proximity-driven scale invariance.

Generalizations of the MSM to weighted[145] and directed[139] networks have also been proposed. The extension to the directed case is

straightforward, because the model does not require geometric distances (which are necessarily symmetric, despite the empirical asymmetry of directed networks) and thus directed networks can be handled by adding another fitness variable per node. With the addition of a third fitness per node, the model can also account for a non-trivial degree of reciprocity[139], thereby replicating a widespread property in real-world directed networks[146–149]. More generally, the fitness variables x_{i_ℓ} can be vectors of arbitrary dimension, with the product $x_{i_\ell}x_{j_\ell}$ in the above expressions interpreted as a scalar product[150,151].

Quenched variant for the renormalization of real-world networks

In the 'quenched' variant of the MSM, the node fitness is interpreted as a deterministic attribute, such as an observable or latent node feature[137,139,150,151]. This variant can therefore model explicitly a real-world network in terms of empirical quantities, as in the family of fitness models[152], or as latent quantities, as in the family of node embedding algorithms[153]. However, whereas generic models in these families are conceived at a fixed resolution level, the MSM describes the same system consistently via the same connection probabilities at all levels of aggregation, with renormalized parameters. It is therefore the only additive fitness model that remains a fitness model upon aggregation[137,150] and, at the same time, a method that produces consistent node embeddings across arbitrary coarse-grainings[151].

The model successfully replicates, at several hierarchical levels, the properties of the international trade network[137,139] (where the fitness is identified with the empirical gross domestic product of countries, and the dyadic factors are identified with geographic distances described by $f(d) = d^{-1}$) and of inter-firm[150] and input–output[151] networks (where the out-ward and in-ward fitnesses are defined as the total output and total input of a firm or industry respectively, and $f \equiv 1$). When the dyadic and/or fitness quantities are taken as input from the data, only the global parameter of the model is left as a free parameter. The latter can be fitted at a specific level of resolution, while providing predictions at all other levels. These multiscale predictions are in very good agreement with the empirical network properties at multiple levels[137,139,150] (Fig. 3b).

Note that the model can cope with extremely uneven aggregation schemes where other methods would fail: for instance, in a production network, some nodes may represent individual firms in one European Union (EU) country, other nodes may represent entire remaining EU countries (with all firms in each country being aggregated into a single node), and yet another 'rest of the world' node may represent all the non-EU countries lumped together[150].

Of course there is no guarantee that, for generic real-world networks, empirical node features exist that can be identified with the additive fitness variables in the MSM. On the other hand, in such a situation the fitness variables can be interpreted as free parameters (in general, vectors of given dimensionality) to be fitted optimally only from the knowledge of the empirical network[151]. This procedure generates node embeddings that represent nodes in an abstract vector space, such that the vector sum represents the merging of nodes[151]. The open challenges in this direction remain the determination of the optimal dimensionality of the embedding vectors, as well as the uniqueness of the latter.

Annealed variant for clustered scale-free networks and fine-graining

In the annealed variant[137,138], the node fitness is considered to be a random variable, as in the family of inhomogeneous random graphs[154]. Hence it acts as a 'latent' variable with no association to a specific real-world feature. In this approach, the requirement of aggregation invariance is applied also to the fitness: at any hierarchical level ℓ, one should be able to draw the node fitnesses from the same probability density function, without having to 'know' their values (or density function) at finer levels. Because the fitness is additive, this requirement immediately implies that it should be an α-stable random variable[141], which means that its density function decays as $x^{-1-\alpha}$ for large x. To ensure the necessary positivity of the fitness, the exponent should be in the range $\alpha \in (0,1)$, which implies a diverging mean (and all higher moments) for the fitness. The only known α-stable distribution in this range is the Lévy distribution ($\alpha = 1/2$), but rigorous results can be derived for any value of α and are largely independent of it[138]. If nodes are aggregated into blocks of equal size, the fitness retains the same density function, up to a rescaling of global parameters only. In its annealed variant, the MSM can generate arbitrarily large networks, and indeed its properties can be studied in the asymptotic limit of a diverging number of nodes[138].

The infinite-mean nature of the fitness makes the expected topological properties of the annealed MSM very different from those produced by similar models with finite-mean fitness. In particular, it can be shown rigorously[137,138] that the expected degree distribution $P(k)$ has a universal power-law tail decay as k^{-2}, irrespective of the value of α. For an aggregation level ℓ into N_ℓ nodes such that $\delta \sim N_\ell^{-1/\alpha}$, such decay is a pure power law[138]; for coarser aggregations, a density-dependent cut-off emerges in the tail[137]. Remarkably, the annealed model displays many realistic network properties, including a decaying assortativity profile, a vanishing global clustering coefficient and a non-vanishing local clustering coefficient in the sparse (vanishing density) regime. A non-vanishing local clustering coefficient is not found in other sparse edge-independent models, unless they are assumed to depend on metric distances; therefore the finding that infinite-mean fitness can generate positive local clustering even without geometry is a relevant insight of the annealed MSM.

Finally, because α-stable random variables are infinitely divisible (that is, they can be expressed as the sum of an arbitrary number of independent identically distributed (i.i.d.) random variables from the same family), in the annealed approach one can fine-grain nodes indefinitely into subnodes, each with its own i.i.d. fitness. This means that in this case the renormalization flow defines not only a semigroup that proceeds bottom-up, but also a group that proceeds in both directions[137]. The open challenge is how to turn this intriguing theoretical property of the model into a practical tool for fine-graining real-world networks that can only be observed at a coarse-grained level, because nodes in real networks may not be characterized by α-stable variables.

Outlook

Although some of the approaches towards network renormalization so far have made notable progress towards formulating a generalized framework for geometric and ensemble heterogeneity, several challenges and open questions remain, which we discuss here.

Resolution level

In real-world network realizations, heterogeneous topologies make it challenging to categorize the geometric and topological organization into 'functional units'. Doing so is less straightforward than for homogeneous lattices or regular trees. Moreover, in several network representations of real-world systems, the available resolution scale

that defines the nodes of the network is typically not intrinsic to the system but derived from observational limitations or the coarseness of data aggregation. For instance, confidentiality issues render inaccessible the individual links in networks of financial relationships (such as interbank loans and exposures) and economic relationships (such as supply and trade), and the absence of complete knowledge of physical person-to-person contacts makes epidemic networks only partly available. Ideally, one would like to ascertain and distinguish characteristic scales that are intrinsic to the properties of the network from those associated to data resolution.

Compatible renormalization of dynamical processes

A major challenge is to renormalize dynamical structures and processes on arbitrary networks in a way that is compatible with the renormalization of the underlying graph structure and ensemble randomness. Previous studies addressing this issue are restricted to processes on regular and/or fractal lattices for which the structural part of the coarse-graining can be defined quite naturally.

In particular, exact RG calculations have been applied to Gaussian fields[155] and random walks[156] on fractal networks, and have been extended to study the fixed points of the Ising model on Hanoi networks[157], revealing distinct critical non-universal behaviours across different regimes. The critical behaviour of percolation on a network growth model has been explored using decimation techniques, showing deviations from the behaviour observed in uncorrelated networks[158]. Real-world systems have also been investigated with these methods. For example, a phenomenological coarse-graining procedure has been developed for activity in neuronal networks. Application to cells in the hippocampus reveal scaling in both static and dynamic quantities, indicating a non-trivial fixed point in the collective behaviour of the network[159].

In general, we expect structural inhomogeneities in real-world networks and their coarse-grained versions to imply a coupling between the renormalization of the dynamical process and that of the topology. The development of a scheme-independent framework that compatibly renormalizes both network dynamics and the underlying geometric or ensemble structure remains a challenge.

Generalized criticality?

Strong heterogeneity and non-locality of connections in real-world networks can affect transition properties between localized and collective excitations close to critical points of dynamical models. They can also give rise to more complex behaviour that necessitate more encompassing definitions of criticality. For instance, one can expect that in epidemic spread on a real contact network, there can be more complex transitions between a collective epidemic state and a localized one than there are on idealizations of contact networks that approximate a lattice. There may be an entire region of interaction parameters in which critical behaviour appears progressively in collective subnetworks that are macroscopic but partial; the appearance of such a parameter region is governed by the strong topological heterogeneity and the possible underlying hierarchical structure. This phenomenon suggests that topological complexity can give rise to a need for an extension of the concept of critical point into something that is somewhat similar to a Griffith phase[160,161].

Parameter relevance and irrelevance from an information-theoretic perspective

Coarse-graining implies information loss. Far from being a drawback, this loss is the very workhorse of RG techniques because it makes it possible to identify the most relevant parameters that describe the behaviour of the system at the largest spatial and temporal scales. Renormalization techniques were originally devised to study physical systems with a large number of degrees of freedom and to identify how the parameters describing the system flow from microscopic to macroscopic scales. A crucial aspect of this flow is how some parameters increase in their relevance to the behaviour of the system as one goes to larger scales, whereas others become more and more irrelevant. In the context of complex networks, studying this parameter flow from the bottom up can provide a first-principles understanding of which quantities and control parameters are the most important at the largest spatial and temporal scales. A complementary top-down approach can also be arrived at from a purely empirical perspective via information theory: Fisher information and the formalism of information geometry applied to the study of complex networks.

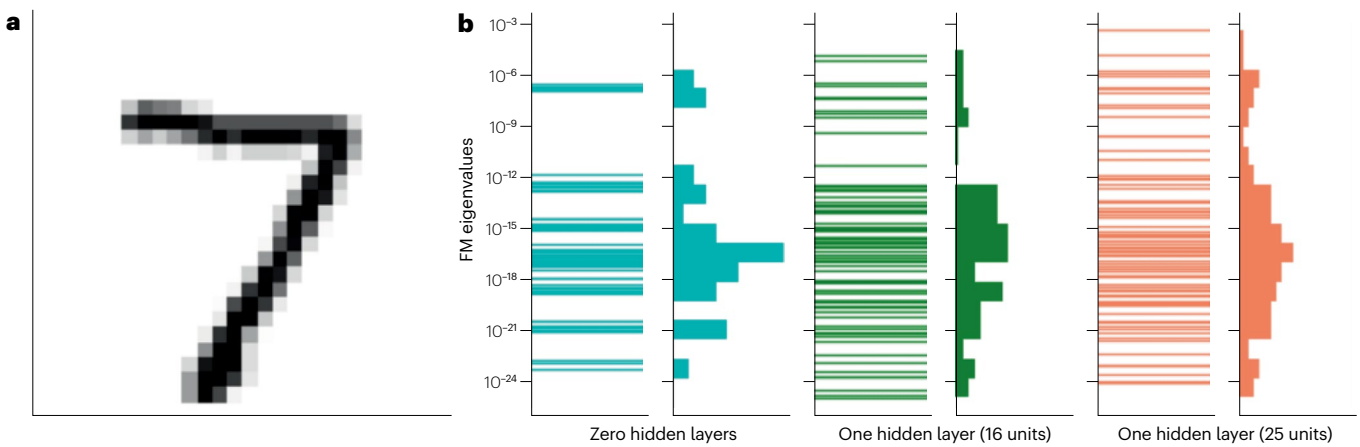

Fig. 4 | Information-theoretic parameter flow. a, An instance of the handwritten numeral 7 from the MNIST (Modified National Institute of Standards and Technology) data set. **b**, Eigenvalues of the Fisher information matrix of 30 trained neural networks that successfully classified the left figure from the MNIST data set (left), and their binned density histogram (right). An exponential eigenvalue hierarchy is evident, implying that only a handful of collective weights are relevant for the accuracy of the trained network. Figure courtesy of Leone Luzzatto.

The concept of parameter relevance in physical systems — encapsulated by the notion of power counting renormalizability in the context of field theories and their hydrodynamic limits — roughly tracks a derivative expansion in all possible terms that could describe the dynamics of the system. That is, one effectively makes a Taylor expansion in theory space, where immediate features become apparent. At large enough scales, terms involving higher derivatives contribute decreasingly to physical observables. From an information-theoretic perspective, this implies that the outcome of an ensemble of observations depends more sensitively on the coefficients of the leading-order terms in any derivative expansion. Hence, a direct transcription of notions of parameter relevance is available in terms of information-theoretic quantities that, moreover, generalize beyond physical systems. Such a translation is not only of immediate conceptual use, but also opens a portal towards identifying and understanding the behaviour of parameters that determine the behaviour of an arbitrary system at the largest scales even in the absence of a microscopic model description, or when dealing with arbitrary geometric and ensemble randomness.

Information geometry and parameter flow

Given any collection of data, one can construct the function giving the likelihood for this data to have been realized by a hypothesized model construction. Maximum-likelihood estimation consists of identifying the parameter set that maximizes this likelihood as being the best inference of what the underlying model might be. How this likelihood varies away from this maximum is captured by the second derivatives of the log likelihood with respect to the parameters that model it, which very naturally has the structure of a metric that captures distances in parameter space. This geometrization of inference, known as information geometry[162], makes it possible to reimagine statistical (Bayesian) inference and renormalization in a unified framework of parameter flow[163].

The Fisher information metric associated with the likelihood constructed from a given data set has a pronounced hierarchy of eigenvalues. This hierarchy implies that small changes in the parameters corresponding to the largest eigenvalues have the largest effect on observed outcomes (Fig. 4), the meaning of which maps directly onto the concept of parameter relevance in the RG sense, with the most relevant parameters corresponding to the largest eigenvalues[164]. It is why, given limited access to information about a system, simple models often tend to do unreasonably well in capturing most of the relevant features. In a neural network trained to recognize handwritten digits (Fig. 4), the collective weights corresponding to the largest eigenvalues of the Fisher information almost entirely dictate the test accuracy of the trained network, with all other parameters and combinations of weights being effectively irrelevant. The sloppy model framework[165] consists of identifying these parameters through the hierarchical structure of the eigenvalues of the Fisher information.

As one successively coarse-grains data sets of a network or simulated realizations of a model embedding, the coarse-grained likelihood results in some eigenvalues increasing in relevance and some decreasing in a manner that maps exactly onto RG relevance. With this knowledge, one can systematically infer the existence of different phases and control parameters from data alone by studying parameter flow under successive coarse-graining of the data, where the only assumptions are the choice of coarse-graining scheme, how to parameterize the underlying geometric or ensemble randomness and the priors assigned to them. This same methodology has been used to identify different phases in heterogeneous chemical systems[166] and would be a promising avenue to pursue in the context of complex networks.

Published online: 26 March 2025

References

1. Pósfai, M. & Barabási, A.-L. *Network Science* (Cambridge Univ. Press, 2016).
2. Squartini, T. & Garlaschelli, D. *Maximum-Entropy Networks: Pattern Detection, Network Reconstruction and Graph Combinatorics* (Springer, 2017).
3. Newman, M. *Networks* (Oxford Univ. Press, 2018).
4. Cimini, G. et al. The statistical physics of real-world networks. *Nat. Rev. Phys.* **1**, 58–71 (2019).
5. Radicchi, F., Ramasco, J., Barrat, A. & Fortunato, S. Complex networks renormalization: flows and fixed points. *Phys. Rev. Lett.* **101**, 3–6 (2008).
6. Radicchi, F., Barrat, A., Fortunato, S. & Ramasco, J. J. Renormalization flows in complex networks. *Phys. Rev. E* **79**, 026104 (2009).
7. Chen, D., Su, H., Wang, X., Pan, G.-J. & Chen, G. Finite-size scaling of geometric renormalization flows in complex networks. *Phys. Rev. E* **104**, 034304 (2021).
8. Chen, D., Cai, D. & Su, H. Scaling properties of scale-free networks in degree-thresholding renormalization flows. *IEEE Trans. Netw. Sci. Eng.* **10**, 3519–3528 (2023).
9. Serafino, M. et al. True scale-free networks hidden by finite size effects. *Proc. Natl Acad. Sci. USA* **118**, e2013825118 (2021).
10. Itzykson, C. & Drouffe, J. M. *Statistical Field Theory: Volume 1, From Brownian Motion to Renormalization and Lattice Gauge Theory* (Cambridge Univ. Press, 1989).
11. Burgess, C. P. *Introduction to Effective Field Theory* (Cambridge Univ. Press, 2020).
12. Bardoscia, M. et al. The physics of financial networks. *Nat. Rev. Phys.* **3**, 490–507 (2021).
13. Soriano-Paños, D. et al. Modeling communicable diseases, human mobility, and epidemics: a review. *Ann. Phys.* **534**, 2100482 (2022).
14. Song, C., Havlin, S. & Makse, H. A. Self-similarity of complex networks. *Nature* **433**, 392–395 (2005).
15. Binder, K. & Young, A. P. Spin glasses: experimental facts, theoretical concepts, and open questions. *Rev. Mod. Phys.* **58**, 801 (1986).
16. Bar-Yam, Y. & Patil, S. P. Renormalization of sparse disorder in the Ising model. Preprint at https://arxiv.org/abs/1805.12556 (2018).
17. Mandelbrot, B. B. *The Fractal Geometry of Nature* Vol. 2 (Freeman, 1982).
18. Samsel, M., Makulski, K., Łepek, M., Fronczak, A. & Fronczak, P. Towards fractal origins of the community structure in complex networks: a model-based approach. Preprint at https://arxiv.org/abs/2309.11126 (2023).
19. Goh, K.-I., Salvi, G., Kahng, B. & Kim, D. Skeleton and fractal scaling in complex networks. *Phys. Rev. Lett.* **96**, 018701 (2006).
20. Kim, J. S., Goh, K.-I., Kahng, B. & Kim, D. Fractality and self-similarity in scale-free networks. *New J. Phys.* **9**, 177 (2007).
21. Fronczak, A. et al. Scaling theory of fractal complex networks. *Sci. Rep.* https://doi.org/10.1038/s41598-024-59765-2 (2024).
22. Song, C., Havlin, S. & Makse, H. A. Origins of fractality in the growth of complex networks. *Nat. Phys.* **2**, 275–281 (2006).
23. Rozenfeld, H. D., Song, C. & Makse, H. A. Small-world to fractal transition in complex networks: a renormalization group approach. *Phys. Rev. Lett.* **104**, 025701 (2010).
24. Newman, M. & Watts, D. Renormalization group analysis of the small-world network model. *Phys. Lett. A* **263**, 341–346 (1999).
25. Kim, B. J. Geographical coarse graining of complex networks. *Phys. Rev. Lett.* **93**, 168701 (2004).
26. Gfeller, D. & De Los Rios, P. Spectral coarse graining of complex networks. *Phys. Rev. Lett.* **99**, 038701 (2007).
27. Wang, Y., Zeng, A., Di, Z. & Fan, Y. Spectral coarse graining for random walks in bipartite networks. *Chaos* **23**, 013104 (2013).
28. Gfeller, D. & De Los Rios, P. Spectral coarse graining and synchronization in oscillator networks. *Phys. Rev. Lett.* **100**, 174104 (2008).
29. Chen, J., an Lu, J., Lu, X., Wu, X. & Chen, G. Spectral coarse graining of complex clustered networks. *Commun. Nonlinear Sci. Numer. Simul.* **18**, 3036–3045 (2013).
30. Jia, Z., Zeng, L., Wang, Y.-Y. & Wang, P. Optimization algorithms for spectral coarse-graining of complex networks. *Physica A* **514**, 925–935 (2019).
31. Zeng, A. & Lü, L. Coarse graining for synchronization in directed networks. *Phys. Rev. E* **83**, 056123 (2011).
32. Wang, P. & Xu, S. Spectral coarse grained controllability of complex networks. *Physica A* **478**, 168–176 (2017).
33. Aygün, E. & Erzan, A. Spectral renormalization group theory on networks. *J. Phys. Conf. Ser.* **319**, 012007 (2011).
34. Tuncer, A. & Erzan, A. Spectral renormalization group for the Gaussian model and ψ^4 theory on nonspatial networks. *Phys. Rev. E* **92**, 022106 (2015).
35. Villegas, P., Gili, T., Caldarelli, G. & Gabrielli, A. Laplacian renormalization group for heterogeneous networks. *Nat. Phys.* **19**, 445–450 (2023).
36. Chen, H., Hou, Z., Xin, H. & Yan, Y. Statistically consistent coarse-grained simulations for critical phenomena in complex networks. *Phys. Rev. E* **82**, 011107 (2010).
37. Long, Y.-S., Jia, Z. & Wang, Y.-Y. Coarse graining method based on generalized degree in complex network. *Physica A* **505**, 655–665 (2018).
38. Wang, Y. et al. Coarse graining method based on node similarity in complex network. *Commun. Netw.* **10**, 51 (2018).

39. Lorrain, F. & White, H. C. Structural equivalence of individuals in social networks. *J. Math. Sociol.* **1**, 49–80 (1971).
40. Dunne, J. A. Food webs. In *Encyclopedia of Complexity and Systems Science* (ed. Meyers, R.) 3661–3682 (Springer, 2009).
41. Itzkovitz, S. et al. Coarse-graining and self-dissimilarity of complex networks. *Phys. Rev. E* **71**, 016127 (2005).
42. Serrano, M. Á., Krioukov, D. & Boguñá, M. Self-similarity of complex networks and hidden metric spaces. *Phys. Rev. Lett.* **100**, 078701 (2008).
43. Alvarez-Hamelin, J., Dall'Asta, L., Barrat, A. & Vespignani, A. K-core decomposition of Internet graphs: hierarchies, self-similarity and measurement biases. *Netw. Heterog. Media* **3**, 371–393 (2008).
44. Lambiotte, R. Multi-scale modularity in complex networks. In *8th International Symposium on Modeling and Optimization in Mobile, Ad Hoc, and Wireless Networks* 546–553 (IEEE, 2010).
45. Karypis, G. & Kumar, V. A fast and high quality multilevel scheme for partitioning irregular graphs. *SIAM J. Sci. Comput.* **20**, 359–392 (1998).
46. Abou-Rjeili, A. & Karypis, G. Multilevel algorithms for partitioning power-law graphs. In *Proc. 20th IEEE International Parallel & Distributed Processing Symposium* https://doi.org/10.1109/IPDPS.2006.1639360 (IEEE, 2006).
47. Leifer, I., Phillips, D., Sorrentino, F. & Makse, H. A. Symmetry-driven network reconstruction through pseudobalanced coloring optimization. *J. Stat. Mech.* **2022**, 073403 (2022).
48. Boldi, P. & Vigna, S. Fibrations of graphs. *Discrete Math.* **243**, 21–66 (2002).
49. Cardelli, L., Tribastone, M., Tschaikowski, M. & Vandin, A. Maximal aggregation of polynomial dynamical systems. *Proc. Natl Acad. Sci. USA* **114**, 10029–10034 (2017).
50. Cardelli, L., Tribastone, M., Tschaikowski, M. & Vandin, A. Erode: a tool for the evaluation and reduction of ordinary differential equations. In *Proc. Tools and Algorithms for the Construction and Analysis of Systems: 23rd International Conference, TACAS 2017* Part II 23, 310–328 (Springer, 2017).
51. Argyris, G. A., Lluch Lafuente, A., Tribastone, M., Tschaikowski, M. & Vandin, A. Reducing Boolean networks with backward equivalence. *BMC Bioinformatics* **24**, 212 (2023).
52. Morone, F., Leifer, I. & Makse, H. A. Fibration symmetries uncover the building blocks of biological networks. *Proc. Natl Acad. Sci. USA* **117**, 8306–8314 (2020).
53. Gili, T. et al. Fibration symmetry-breaking supports functional transitions in a brain network engaged in language. Preprint at https://arxiv.org/abs/2409.02674 (2024).
54. Papadopoulos, F., Psounis, K. & Govindan, R. Performance preserving topological downscaling of internet-like networks. *IEEE J. Sel. Areas Commun.* **24**, 2313–2326 (2006).
55. Papadopoulos, F. & Psounis, K. Efficient identification of uncongested internet links for topology downscaling. *SIGCOMM Comput. Commun. Rev.* **37**, 39–52 (2007).
56. Di, X., Zhao, Y., Huang, S. & Liu, H. X. A similitude theory for modeling traffic flow dynamics. *IEEE Trans. Intell. Transp. Syst.* **20**, 900–911 (2019).
57. Chen, H., Perozzi, B., Hu, Y. & Skiena, S. HARP: hierarchical representation learning for networks. In *Proc. 32nd AAAI Conference on Artificial Intelligence/30th Innovative Applications of Artificial Intelligence Conference/8th AAAI Symposium on Educational Advances in Artificial Intelligence (AAAI'18/IAAI'18/EAAI'18)* 2127–2134 (AAAI, 2018).
58. Loukas, A. Graph reduction with spectral and cut guarantees. *J. Mach. Learn. Res.* **20**, 1–42 (2019).
59. Jin, Y., Loukas, A. & JaJa, J. Graph coarsening with preserved spectral properties. In *Proc. International Conference on Artificial Intelligence and Statistics* 4452–4462 (PMLR, 2020).
60. Fahrbach, M., Goranci, G., Peng, R., Sachdeva, S. & Wang, C. Faster graph embeddings via coarsening. In *Proc. International Conference on Machine Learning* 2953–2963 (PMLR, 2020).
61. Liang, J., Gurukar, S. & Parthasarathy, S. MILE: A multi-level framework for scalable graph embedding. In *Proc. International AAAI Conference on Web and Social Media* Vol. 15, 361–372 (AAAI, 2021).
62. Huang, Z., Zhang, S., Xi, C., Liu, T. & Zhou, M. Scaling up graph neural networks via graph coarsening. In *Proc. 27th ACM SIGKDD Conference on Knowledge Discovery and Data Mining* 675–684 (ACM, 2021).
63. Zhang, Z., Ghavasieh, A., Zhang, J. & De Domenico, M. Coarse-graining network flow through statistical physics and machine learning. *Nat. Commun.* **16**, 1605 (2025).
64. Yedidia, J. S. & Bouchaud, J.-P. Renormalization group approach to error-correcting codes. *J. Phys. A* **36**, 1267 (2003).
65. Klein, B. & Hoel, E. The emergence of informative higher scales in complex networks. *Complexity* **2020**, 1–12 (2020).
66. Faccin, M., Schaub, M. T. & Delvenne, J.-C. Entrograms and coarse graining of dynamics on complex networks. *J. Complex Netw.* **6**, 661–678 (2017).
67. Boguñá, M. et al. Network geometry. *Nat. Rev. Phys.* **3**, 114–135 (2021).
68. García-Pérez, G., Boguñá, M. & Serrano, M. Á. Multiscale unfolding of real networks by geometric renormalization. *Nat. Phys.* **14**, 583–589 (2018).
69. Zheng, M., García-Pérez, G., Boguñá, M. & Serrano, M. Á. Scaling up real networks by geometric branching growth. *Proc. Natl Acad. Sci. USA* https://doi.org/10.1073/pnas.2018994118 (2021).
70. Zheng, M., García-Pérez, G., Boguñá, M. & Serrano, M. Á. Geometric renormalization of weighted networks. *Commun. Phys.* **7**, 97 (2024).
71. van der Kolk, J., Serrano, M. & Boguñá, M. Renormalization of networks with weak geometric coupling. *Phys. Rev. E* **110**, L032302 (2024).
72. Krioukov, D., Papadopoulos, F., Kitsak, M., Vahdat, A. & Boguñá, M. Hyperbolic geometry of complex networks. *Phys. Rev. E* **82**, 036106 (2010).
73. Gilbert, E. N. Random plane networks. *J. Soc. Indust. Appl. Math.* **9**, 533–543 (1961).
74. Penrose, M. *Random Geometric Graphs* Vol. 5 (Oxford Univ. Press, 2003).
75. Hoff, P. D., Raftery, A. E. & Handcock, M. S. Latent space approaches to social network analysis. *J. Am. Stat. Assoc.* **97**, 1090–1098 (2002).
76. Boguñá, M., Krioukov, D., Almagro, P. & Serrano, M. Á. Small worlds and clustering in spatial networks. *Phys. Rev. Res.* **2**, 023040 (2020).
77. van der Kolk, J., Serrano, M. Á. & Boguñá, M. An anomalous topological phase transition in spatial random graphs. *Commun. Phys.* **5**, 245 (2022).
78. van der Kolk, J., Serrano, M. Á. & Boguñá, M. Random graphs and real networks with weak geometric coupling. *Phys. Rev. Res.* **6**, 013337 (2024).
79. García-Pérez, G., Allard, A., Serrano, M. Á. & Boguñá, M. Mercator: uncovering faithful hyperbolic embeddings of complex networks. *New J. Phys.* **21**, 123033 (2019).
80. Jankowski, R., Allard, A., Boguñá, M. & Serrano, M. Á. The *D*-Mercator method for the multidimensional hyperbolic embedding of real networks. *Nat. Commun.* **14**, 7585 (2023).
81. Boguñá, M., Papadopoulos, F. & Krioukov, D. Sustaining the internet with hyperbolic mapping. *Nat. Commun.* **1**, 62 (2010).
82. Gugelmann, L., Panagiotou, K. & Peter, U. Random hyperbolic graphs: degree sequence and clustering. In *Proc. Automata, Languages and Programming, 39th International Colloquium (ICALP 2012)* (eds Czumaj, A. et al.) 573–585 (Springer, 2012).
83. Candellero, E. & Fountoulakis, N. Clustering and the hyperbolic geometry of complex networks. *Internet Math.* **12**, 2–53 (2016).
84. Fountoulakis, N., van der Hoorn, P., Müller, T. & Schepers, M. Clustering in a hyperbolic model of complex networks. *Electron. J. Probab.* **26**, 1–132 (2021).
85. Abdullah, M. A., Fountoulakis, N. & Bode, M. ypical distances in a geometric model for complex networks. *Internet Math.* https://doi.org/10.24166/im.13.2017 (2017).
86. Friedrich, T. & Krohmer, A. On the diameter of hyperbolic random graphs. *SIAM J. Discrete Math.* **32**, 1314–1334 (2018).
87. Müller, T. & Staps, M. The diameter of KPKVB random graphs. *Adv. Appl. Probab.* **51**, 358–377 (2019).
88. Serrano, M. Á., Krioukov, D. & Boguñá, M. Percolation in self-similar networks. *Phys. Rev. Lett.* **106**, 048701 (2011).
89. Fountoulakis, N. & Müller, T. Law of large numbers for the largest component in a hyperbolic model of complex networks. *Ann. Appl. Probab.* **28**, 607–650 (2018).
90. Bianconi, G. & Ziff, R. Topological percolation on hyperbolic simplicial complexes. *Phys. Rev. E* **98**, 052308 (2018).
91. Kiwi, M. & Mitsche, D. Spectral gap of random hyperbolic graphs and related parameters. *Ann. Appl. Probab.* **28**, 941–989 (2018).
92. Papadopoulos, F., Kitsak, M., Serrano, M. Á., Boguñá, M. & Krioukov, D. Popularity versus similarity in growing networks. *Nature* **489**, 537–540 (2012).
93. Allard, A., Serrano, M. Á., García-Pérez, G. & Boguñá, M. The geometric nature of weights in real complex networks. *Nat. Commun.* **8**, 14103 (2017).
94. Serrano, M. Á., Boguñá, M. & Sagués, F. Uncovering the hidden geometry behind metabolic networks. *Mol. Biosyst.* **8**, 843 (2012).
95. Kitsak, M., Papadopoulos, F. & Krioukov, D. Latent geometry of bipartite networks. *Phys. Rev. E* **95**, 032309 (2017).
96. Budel, G. & Kitsak, M. Complementarity in complex networks. Preprint at https://arxiv.org/abs/2003.06665 (2023).
97. Kleineberg, K.-K., Boguñá, M., Serrano, M. Á. & Papadopoulos, F. Hidden geometric correlations in real multiplex networks. *Nat. Phys.* **12**, 1076–1081 (2016).
98. Kleineberg, K.-K., Buzna, L., Papadopoulos, F., Boguñá, M. & Serrano, M. Á. Geometric correlations mitigate the extreme vulnerability of multiplex networks against targeted attacks. *Phys. Rev. Lett.* **118**, 218301 (2017).
99. Zuev, K., Boguñá, M., Bianconi, G. & Krioukov, D. Emergence of soft communities from geometric preferential attachment. *Sci. Rep.* **5**, 9421 (2015).
100. García-Pérez, G., Serrano, M. Á. & Boguñá, M. Soft communities in similarity space. *J. Stat. Phys.* **173**, 775–782 (2018).
101. Muscoloni, A. & Cannistraci, C. V. A nonuniform popularity-similarity optimization (nPSO) model to efficiently generate realistic complex networks with communities. *New. J. Phys.* **20**, 052002 (2018).
102. Allard, A., Serrano, M. Á. & Boguñá, M. Geometric description of clustering in directed networks. *Nat. Phys.* **20**, 150–156 (2024).
103. Aliakbarisani, R., Ángeles Serrano, M. & Boguñá, M. Feature-enriched hyperbolic network geometry. Preprint at https://arxiv.org/abs/2307.14198 (2023).
104. Zheng, M., Allard, A., Hagmann, P., Alemán-Gómez, Y. & Serrano, M. Á. Geometric renormalization unravels self-similarity of the multiscale human connectome. *Proc. Natl Acad. Sci. USA* **117**, 20244–20253 (2020).
105. Barrat, A., Barthelemy, M., Pastor-Satorras, R. & Vespignani, A. The architecture of complex weighted networks. *Proc. Natl Acad. Sci. USA* **101**, 3747–3752 (2004).
106. Serrano, M. Á., Boguñá, M. & Pastor-Satorras, R. Correlations in weighted networks. *Phys. Rev. E* **74**, 055101 (2006).
107. Nolan, J. P. *Univariate Stable Distributions: Models for Heavy Tailed Data* (Springer, 2020).
108. Caldarelli, G., Gabrielli, A., Gili, T. & Villegas, P. Laplacian renormalization group: an introduction to heterogeneous coarse-graining. *J. Stat. Mech.* **2024**, 084002 (2024).
109. De Domenico, M. & Biamonte, J. Spectral entropies as information-theoretic tools for complex network comparison. *Phys. Rev. X* **6**, 041062 (2016).
110. Masuda, N., Porter, M. A. & Lambiotte, R. Random walks and diffusion on networks. *Phys. Rep.* **716**, 1–58 (2017).
111. Kadanoff, L. P. Notes on Migdal's recursion formulas. *Ann. Phys.* **100**, 359–394 (1976).
112. Migdal, A. A. Phase transitions in gauge and spin-lattice systems. *Zh. Eksp. Teor. Fiz.* **69**, 1457–1465 (1975).

113. Wilson, K. G. & Kogut, J. The renormalization group and the ε expansion. *Phys. Rep.* **12**, 75–199 (1974).
114. Newman, M. E. J. *Networks: An Introduction* (Oxford Univ. Press, 2010).
115. Moretti, P. & Zaiser, M. Network analysis predicts failure of materials and structures. *Proc. Natl Acad. Sci. USA* **116**, 16666–16668 (2019).
116. Burioni, R. & Cassi, D. Random walks on graphs: ideas, techniques and results. *J. Phys. A* **38**, R45–R78 (2005).
117. Villegas, P., Gabrielli, A., Poggialini, A. & Gili, T. Multi-scale Laplacian community detection in heterogeneous networks. *Phys. Rev. Res.* **7**, 013065 (2025).
118. Kadanoff, L. P. Scaling laws for Ising models near T_c. *Phys. Phys. Fiz.* **2**, 263–272 (1966).
119. Wilson, K. G. Problems in physics with many scales of length. *Sci. Am.* **241**, 158–179 (1979).
120. Hinrichsen, H. Non-equilibrium critical phenomena and phase transitions into absorbing states. *Adv. Phys.* **49**, 815–958 (2000).
121. Dornic, I., Chaté, H. & Muñoz, M. A. Integration of Langevin equations with multiplicative noise and the viability of field theories for absorbing phase transitions. *Phys. Rev. Lett.* **94**, 100601 (2005).
122. Burioni, R. & Cassi, D. Geometrical universality in vibrational dynamics. *Mod. Phys. Lett. B* **11**, 1095–1101 (1997).
123. Cassi, D. Phase transitions and random walks on graphs: a generalization of the Mermin–Wagner theorem to disordered lattices, fractals, and other discrete structures. *Phys. Rev. Lett.* **68**, 3631–3634 (1992).
124. Reitz, M. & Bianconi, G. The higher-order spectrum of simplicial complexes: a renormalization group approach. *J. Phys. A* **53**, 295001 (2020).
125. Bianconi, G. & Dorogovstev, S. N. The spectral dimension of simplicial complexes: a renormalization group theory. *J. Stat. Mech.* **2020**, 014005 (2020).
126. Nurisso, M. et al. Higher-order Laplacian renormalization. *Nat. Phys.* https://doi.org/10.1038/s41567-025-02784-1 (2025).
127. Cheng, A., Xu, Y., Sun, P. & Tian, Y. A simplex path integral and a simplex renormalization group for high-order interactions. *Rep. Prog. Phys.* **87**, 087601 (2024).
128. Ghavasieh, A., Nicolini, C. & De Domenico, M. Statistical physics of complex information dynamics. *Phys. Rev. E* **102**, 052304 (2020).
129. Villegas, P., Gabrielli, A., Santucci, F., Caldarelli, G. & Gili, T. Laplacian paths in complex networks: information core emerges from entropic transitions. *Phys. Rev. Res.* **4**, 033196 (2022).
130. Binney, J. J, Dowrick, N. J, Fisher, A. J & Newman, M. E. *The Theory of Critical Phenomena: An Introduction to the Renormalization Group* (Oxford Univ. Press, 1992).
131. Pathria, R. K. & Beale, P. D. *Statistical Mechanics* (Academic Press, 2011).
132. Holland, P. W., Laskey, K. B. & Leinhardt, S. Stochastic blockmodels: first steps. *Soc. Networks* **5**, 109 (1983).
133. Burioni, R. & Cassi, D. Universal properties of spectral dimension. *Phys. Rev. Lett.* **76**, 1091–1093 (1996).
134. Moretti, P. & Muñoz, M. A. Griffiths phases and the stretching of criticality in brain networks. *Nat. Commun.* **4**, 2521 (2013).
135. Poggialini, A., Villegas, P., Muñoz, M. A. & Gabrielli, A. Networks with many structural scales: a renormalization group perspective. *Phys. Rev. Lett.* **134**, 057401 (2024).
136. de C. Loures, M., Piovesana, A. A. & Brum, J. A. Laplacian coarse graining in complex networks. Preprint at https://arxiv.org/abs/2302.07093 (2023).
137. Garuccio, E., Lalli, M. & Garlaschelli, D. Multiscale network renormalization: scale-invariance without geometry. *Phys. Rev. Res.* **5**, 043101 (2023).
138. Avena, L., Garlaschelli, D., Hazra, R. S. & Lalli, M. Inhomogeneous random graphs with infinite-mean fitness variables. Preprint at https://arxiv.org/abs/2212.08462 (2022).
139. Lalli, M. & Garlaschelli, D. Geometry-free renormalization of directed networks: scale-invariance and reciprocity. Preprint at https://arxiv.org/abs/2403.00235 (2024).
140. Uchaikin, V. V. & Zolotarev, V. M. *Chance and Stability: Stable Distributions and their Applications* (Walter de Gruyter, 2011).
141. Samoroditsky, G. & Taqqu, M. S. *Stable Non-Gaussian Random Processes: Stochastic Models with Infinite Variance* (Chapman & Hall, 1994).
142. Lévy, P. L'addition des variables aléatoires définies sur une circonférence. *Bull. Soc. Math. Fr.* **67**, 1–41 (1939).
143. Balkema, A. A. & Resnick, S. I. Max-infinite divisibility. *J. Appl. Probab.* **14**, 309–319 (1977).
144. Giné, E., Hahn, M. G. & Vatan, P. Max-infinitely divisible and max-stable sample continuous processes. *Probab. Theory Relat. Fields* **87**, 139–165 (1990).
145. Verteletskyi, V. *Renormalization of Networks with Weighted Links*. MSc thesis, Leiden Univ. (2022).
146. Garlaschelli, D. & Loffredo, M. I. Patterns of link reciprocity in directed networks. *Phys. Rev. Lett.* **93**, 268701 (2004).
147. Garlaschelli, D. & Loffredo, M. I. Multispecies grand-canonical models for networks with reciprocity. *Phys. Rev. E* **73**, 015101 (2006).
148. Squartini, T., Picciolo, F., Ruzzenenti, F. & Garlaschelli, D. Reciprocity of weighted networks. *Sci. Rep.* **3**, 2729 (2013).
149. Gallo, A., Saracco, F., Lambiotte, R., Garlaschelli, D. & Squartini, T. Patterns of link reciprocity in directed, signed networks. *Phys. Rev. E* **111**, 024312 (2025).
150. Ialongo, L. N., Bangma, S., Jansen, F. & Garlaschelli, D. Multi-scale reconstruction of large supply networks. Preprint at https://arxiv.org/abs/2412.16122 (2024).
151. Milocco, R., Jansen, F. & Garlaschelli, D. Multi-scale node embeddings for graph modeling and generation. Preprint at https://arxiv.org/abs/2412.04354 (2024).
152. Caldarelli, G., Capocci, A., De Los Rios, P. & Munoz, M. A. Scale-free networks from varying vertex intrinsic fitness. *Phys. Rev. Lett.* **89**, 258702 (2002).
153. Dehghan-Kooshkghazi, A., Kamiński, B., Kraiński, Ł., Prałat, P. & Théberge, F. Evaluating node embeddings of complex networks. *J. Complex Netw.* **10**, cnac030 (2022).
154. van der Hofstad, R. *Random Graphs and Complex Networks* (Cambridge Univ. Press, 2024).
155. Hattori, K., Hattori, T. & Watanabe, H. Gaussian field theories on general networks and the spectral dimensions. *Prog. Theor. Phys. Suppl.* **92**, 108–143 (1987).
156. Burioni, R. & Cassi, D. Random walks on graphs: ideas, techniques and results. *J. Phys. A* **38**, R45 (2005).
157. Boettcher, S. & Brunson, C. T. Renormalization group for critical phenomena in complex networks. *Front. Physiol.* **2**, 16081 (2011).
158. Dorogovtsev, S. N. Renormalization group for evolving networks. *Phys. Rev. E* **67**, 045102 (2003).
159. Meshulam, L., Gauthier, J. L., Brody, C. D., Tank, D. W. & Bialek, W. Coarse graining, fixed points, and scaling in a large population of neurons. *Phys. Rev. Lett.* **123**, 178103 (2019).
160. Griffiths, R. B. Nonanalytic behavior above the critical point in a random Ising ferromagnet. *Phys. Rev. Lett.* **23**, 17–19 (1969).
161. Munoz, M. A., Juhász, R., Castellano, C. & Ódor, G. Griffiths phases on complex networks. *Phys. Rev. Lett.* **105**, 128701 (2010).
162. Amari, S.-i. *Information Geometry and Its Applications* (Springer, 2016).
163. Berman, D. S., Klinger, M. S. & Stapleton, A. G. Bayesian renormalization. *Mach. Learn. Sci. Tech.* **4**, 045011 (2023).
164. Raju, A., Machta, B. B. & Sethna, J. P. Information loss under coarse graining: a geometric approach. *Phys. Rev. E* **98**, 052112 (2018).
165. Machta, B. B., Chachra, R., Transtrum, M. K. & Sethna, J. P. Parameter space compression underlies emergent theories and predictive models. *Science* **342**, 604–607 (2013).
166. Har-Shemesh, O., Quax, R., Hoekstra, A. G. & Sloot, P. M. A. Information geometric analysis of phase transitions in complex patterns: the case of the Gray-Scott reaction–diffusion model. *J. Stat. Mech.* **4**, 043301 (2016).
167. Ehrenfest, P. & Ehrenfest, T. *Begriffliche Grundlagen der statistischen Auffassung in der Mechanik* (Springer, 1907).
168. Niemeijer, T. & van Leeuwen, J. M. J. Wilson theory for spin systems on a triangular lattice. *Phys. Rev. Lett.* **31**, 1411–1414 (1973).
169. Kadanoff, L. P. Variational principles and approximate renormalization group calculations. *Phys. Rev. Lett.* **34**, 1005–1008 (1975).
170. Southern, B. W. Kadanoff's variational renormalisation group method: the Ising model on the square and triangular lattices. *J. Phys. A* **11**, L1 (1978).
171. Jan, N. & Glazer, A. Kadanoff's approximate renormalization group transformation applied to the triangular Ising lattice. *Physica A* **91**, 461–468 (1978).
172. den Nijs, M. & Knops, H. Variational renormalization method and the Potts model. *Physica A* **93**, 441–456 (1978).
173. Di Castro, C. & Jona-Lasinio, G. On the microscopic foundation of scaling laws. *Phys. Lett. A* **29**, 322–323 (1969).
174. Gell-Mann, M. & Low, F. E. Quantum electrodynamics at small distances. *Phys. Rev.* **95**, 1300 (1954).
175. Zinn-Justin, J. *Quantum Field Theory and Critical Phenomena* (Oxford Univ. Press, 2021).
176. Amit, D. J. & Martin-Mayor, V. *Field Theory, the Renormalization Group and Critical Phenomena* (World Scientific, 2005).
177. Täuber, U. C. Renormalization group: applications in statistical physics. *Nucl. Phys. B* **228**, 7–34 (2012).
178. Pelissetto, A. & Vicari, E. Critical phenomena and renormalization-group theory. *Phys. Rep.* **368**, 549–727 (2002).
179. Efrati, E., Wang, Z., Kolan, A. & Kadanoff, L. P. Real-space renormalization in statistical mechanics. *Rev. Mod. Phys.* **86**, 647–667 (2014).
180. Gefen, Y., Mandelbrot, B. B. & Aharony, A. Critical phenomena on fractal lattices. *Phys. Rev. Lett.* **45**, 855 (1980).
181. Gefen, Y., Aharony, A., Mandelbrot, B. B. & Kirkpatrick, S. Solvable fractal family, and its possible relation to the backbone at percolation. *Phys. Rev. Lett.* **47**, 1771 (1981).
182. Phani, M. K. & Dhar, D. Real-space renormalisation group: application to directed percolation. *J. Phys. C* **15**, 1391 (1982).
183. Gefen, Y., Aharony, A. & Mandelbrot, B. B. Phase transitions on fractals. I. Quasi-linear lattices. *J. Phys. A* **16**, 1267 (1983).
184. Gefen, Y., Aharony, A., Shapir, Y. & Mandelbrot, B. B. Phase transitions on fractals. II. Sierpinski gaskets. *J. Phys. A* **17**, 435 (1984).
185. Gefen, Y., Aharony, A. & Mandelbrot, B. B. Phase transitions on fractals. III. Infinitely ramified lattices. *J. Phys. A* **17**, 1277 (1984).
186. Das, D., Dey, S., Jacobsen, J. L. & Dhar, D. Critical behavior of loops and biconnected clusters on fractals of dimension $d<2$. *J. Phys. A* **41**, 485001 (2008).
187. Della Morte, M. & Sannino, F. Renormalization group approach to pandemics as a time-dependent SIR model. *Front. Phys.* https://doi.org/10.3389/fphy.2020.591876 (2021).
188. Cavagna, A. et al. Dynamic scaling in natural swarms. *Nat. Phys.* **13**, 914–918 (2017).
189. Cavagna, A. et al. Dynamical renormalization group approach to the collective behavior of swarms. *Phys. Rev. Lett.* https://doi.org/10.1103/PhysRevLett.123.268001 (2019).
190. Cavagna, A. et al. Natural swarms in 3.99 dimensions. *Nat. Phys.* **19**, 1043–1049 (2023).
191. Koch-Janusz, M. & Ringel, Z. Mutual information, neural networks and the renormalization group. *Nat. Phys.* **14**, 578–582 (2018).
192. Li, S.-H. & Wang, L. Neural network renormalization group. *Phys. Rev. Lett.* https://doi.org/10.1103/PhysRevLett.121.260601 (2018).
193. Hu, H.-Y., Li, S.-H., Wang, L. & You, Y.-Z. Machine learning holographic mapping by neural network renormalization group. *Phys. Rev. Res.* **2**, 023369 (2020).

194. Caso, F., Trappolini, G., Bacciu, A., Liò, P. & Silvestri, F. Renormalized graph neural networks. Preprint at https://arxiv.org/abs/2306.00707 (2023).
195. Young, A. P. & Stinchcombe, R. B. A renormalization group theory for percolation problems. *J. Phys. C* **8**, L535 (1975).
196. Reynolds, P. J., Stanley, H. E. & Klein, W. A real-space renormalization group for site and bond percolation. *J. Phys. C* **10**, L167 (1977).
197. Galam, S. Real space renormalization group and totalitarian paradox of majority rule voting. *Physica A* **285**, 66–76 (2000).
198. Kogan, O., Rogers, J. L., Cross, M. C. & Refael, G. Renormalization group approach to oscillator synchronization. *Phys. Rev. E* **80**, 036206 (2009).
199. Östborn, P. Renormalization of oscillator lattices with disorder. *Phys. Rev. E* **79**, 051114 (2009).
200. Garlaschelli, D., den Hollander, F., Meylahn, J. & Zeegers, B. Synchronization of phase oscillators on the hierarchical lattice. *J. Stat. Phys.* **174**, 188–218 (2019).
201. Levin, M. & Nave, C. P. Tensor renormalization group approach to two-dimensional classical lattice models. *Phys. Rev. Lett.* https://doi.org/10.1103/PhysRevLett.99.120601 (2007).
202. Evenbly, G. & Vidal, G. Tensor network renormalization. *Phys. Rev. Lett.* https://doi.org/10.1103/PhysRevLett.115.180405 (2015).
203. Bal, M., Mariën, M., Haegeman, J. & Verstraete, F. Renormalization group flows of Hamiltonians using tensor networks. *Phys. Rev. Lett.* https://doi.org/10.1103/PhysRevLett.118.250602 (2017).
204. Lenggenhager, P. M., Gökmen, D. E., Ringel, Z., Huber, S. D. & Koch-Janusz, M. Optimal renormalization group transformation from information theory. *Phys. Rev. X* **10**, 011037 (2020).
205. Gökmen, D. E., Ringel, Z., Huber, S. D. & Koch-Janusz, M. Statistical physics through the lens of real-space mutual information. *Phys. Rev. Lett.* **127**, 240603 (2021).
206. Gordon, A., Banerjee, A., Koch-Janusz, M. & Ringel, Z. Relevance in the renormalization group and in information theory. *Phys. Rev. Lett.* **126**, 240601 (2021).
207. Sarra, L., Aiello, A. & Marquardt, F. Renormalized mutual information for artificial scientific discovery. *Phys. Rev. Lett.* **126**, 200601 (2021).
208. Gökmen, D. E., Ringel, Z., Huber, S. D. & Koch-Janusz, M. Symmetries and phase diagrams with real-space mutual information neural estimation. *Phys. Rev. E* **104**, 064106 (2021).
209. Canet, L., Delamotte, B., Deloubrière, O. & Wschebor, N. Nonperturbative renormalization-group study of reaction–diffusion processes. *Phys. Rev. Lett.* **92**, 195703 (2004).
210. Canet, L., Chaté, H. & Delamotte, B. Quantitative phase diagrams of branching and annihilating random walks. *Phys. Rev. Lett.* **92**, 255703 (2004).
211. Canet, L., Chaté, H., Delamotte, B., Dornic, I. & Muñoz, M. A. Nonperturbative fixed point in a nonequilibrium phase transition. *Phys. Rev. Lett.* **95**, 100601 (2005).
212. Canet, L., Chaté, H. & Delamotte, B. General framework of the non-perturbative renormalization group for non-equilibrium steady states. *J. Phys. A* **44**, 495001 (2011).
213. Tarpin, M., Benitez, F., Canet, L. & Wschebor, N. Nonperturbative renormalization group for the diffusive epidemic process. *Phys. Rev. E* **96**, 022137 (2017).

Acknowledgements
D.G. acknowledges support from the European Union (EU), NextGenerationEU National Recovery and Resilience Plan (Piano Nazionale di Ripresa e Resilienza, PNRR) projects 'SoBigData.it — Strengthening the Italian RI for Social Mining and Big Data Analytics' (Grant IR0000013, no. 3264, 28/12/2021) and 'Reconstruction, Resilience and Recovery of Socio-Economic Networks' (RECON-NET EP_FAIR_005 — PE0000013 'FAIR', PNRR M4C2 Investment 1.3). D.G. also acknowledges L. Avena, A. Catanzaro, E. Garuccio, R. Hazra, L. N. Ialongo, F. Jansen, M. Lalli and R. Milocco for scientific collaboration on the subject. A.G. acknowledges the EU, as this work was carried out within the project 'C2T — From Crises to Theory: towards a science of resilience and recovery for economic and financial systems' (CUP: F53D23010380001) — NRRP Mission 4 Component 2 Investment Line 1.1 'Research Projects of National Relevant Interest — PRIN', funded by NextGenerationEU. A.G. also acknowledges P. Villegas, T. Gili and G. Caldarelli for scientific collaboration and discussions. M.A.S. acknowledges support from TED2021-129791B-I00, funded by MICIU/AEI/10.13039/501100011033 and the 'European Union NextGenerationEU/PRTR'; PID2022-137505NB-C22, funded by MICIU/AEI/10.13039/501100011033 and by 'ERDF A way of making Europe'; and 2021SGR00856, funded by Generalitat de Catalunya. M.A.S. thanks M. Boguñá, G. García-Pérez and M. Zheng for scientific collaboration. S.P. thanks Y. Bar-Yam, C. Burgess, A. D. Jackson, K. Grosvenor and L. Luzzatto for scientific collaboration and discussions.

Author contributions
All authors contributed equally to the design and writing of this Technical Review.

Competing interests
The authors declare no competing interests.

Additional information
Supplementary information The online version contains supplementary material available at https://doi.org/10.1038/s42254-025-00817-5.

Peer review information *Nature Review Physics* thanks Konstantin Klemm, Dan Chen and Filippo Radicchi for their contribution to the peer review of this work.

nature reviews physics

https://doi.org/10.1038/s42254-025-00817-5

Supplementary information

Network renormalization

In the format provided by
the authors and unedited

Supplementary Information: Network Renormalization

Andrea Gabrielli[1,2,3], Diego Garlaschelli[4,5,*], Subodh P. Patil[5], and M. Ángeles Serrano[6,7,8]

[1]Dipartimento di Ingegneria Civile, Informatica e delle Tecnologie Aeronautiche, Università degli Studi 'Roma Tre', Via Vito Volterra 62, 00146 - Rome, Italy
[2]'Enrico Fermi' Research Center (CREF), Via Panisperna 89A, 00184 - Rome, Italy
[3]Istituto dei Sistemi Complessi (ISC) - CNR, Rome, Italy
[4]IMT School for Advanced Studies, Piazza S. Francesco 19, 55100 - Lucca, Italy
[5]Lorentz Institute for Theoretical Physics, University of Leiden, The Netherlands
[6]Departament de Física de la Matèria Condensada, Universitat de Barcelona, Spain
[7]Universitat de Barcelona Institute of Complex Systems (UBICS), Spain
[8]ICREA, Barcelona, Spain
[*]Corresponding author: diego.garlaschelli@imtlucca.it

1 Behavior of the average degree under geometric renormalization

As proved in [1], the average degree of complex networks with $\beta > 0$ changes as

$$\langle k \rangle^{(\ell+1)} = r^{\nu} \langle k \rangle^{(\ell)}$$

in the geometric renormalization flow. The scaling factor ν depends on the connectivity properties of the original network. More specifically, it is a function of the exponent γ of the degree distribution and the exponent β quantifying clustering and the coupling between topology and geometry:

- If $0 < \frac{\gamma-1}{\beta} \leq 1$, the flow is dominated by the exponent of the degree distribution γ, and the scaling factor is given by $\nu = \frac{2}{\gamma-1} - 1$.
- If $1 \leq \frac{\gamma-1}{\beta} < 2$, the flow is dominated by the strength of clustering and $\nu = \frac{2}{\beta} - 1$.

Therefore,

- If $\gamma < 3$ or $\beta < 2$, then ν is positive and the model flows towards a highly connected graph.
- The average degree is preserved if $\gamma = 3$ and $\beta \geq 2$, or $\beta = 2$ and $\gamma \geq 3$, which indicates that the network is at the edge of the transition between the small-world and non-small-world phases.
- If $\gamma > 3$ and $\beta > 2$, then ν is negative, causing the RGN flow to produce increasingly sparser networks approaching a unidimensional ring structure as a fixed point. In this case, the renormalized layers eventually lose the small-world property.

Finally, if $\beta < \frac{\gamma-1}{2}$, the degree distribution becomes increasingly homogeneous, revealing that degree heterogeneity is only present at short scales.

2 Extension of the geometric renormalization scheme to weighted networks

The geometric renormalization of weights (GRW) [2] produces the multiscale unfolding of a weighted network into a shell of self-similar layers by imposing the preservation of the relation between the strength and the degree of nodes. First, application of GR ensures self-similarity of the binarized structure of the network. Second, weights are renormalized. The technique for the renormalization of weights is sustained by the renormalizability of the $\mathrm{W}\mathbb{S}^D$ model [3]. In this model, weights between connected nodes in the topology generated by the $\mathbb{S}^D$ model are the result of coupling the weighted structure of the network to the latent metric space. In $D = 1$, the transformation of weights, named ϕ-GRW, is given by a specific choice of the function $\mathcal{G}$ in Eq. (3) in the main text, namely

$$W^{(\ell+1)}_{i_{\ell+1}j_{\ell+1}} = C \left[\sum_{i_\ell \in i_{\ell+1}} \sum_{j_\ell \in j_{\ell+1}} (W^{(\ell)}_{i_\ell j_\ell})^\phi \right]^{1/\phi} ,$$

which takes the form of a ϕ-norm where C is a rescaling factor and ϕ is a parameter that depends on the weighted and unweighted structure of the network. In practice, an effective approximation with practical advantages that retains the semigroup structure property is to select the maximum weight of the renormalized links. This strategy, named sup-GRW, is equivalent to setting $\phi = \infty$ and is effectively reached already for moderate values

of ϕ due to the fast convergence of the ϕ-norm of a set of values to the maximum in the set. As an alternative, sum-GRW renormalizes the weights by their sum [4]. This approach is equivalent to setting $\phi = 1$ and, in general, does not preserve the relation between hidden strength and hidden degree. Weighted networks with heterogeneous degree distributions from very different domains show geometric scaling when coarse-grained and rescaled using ϕ-GRW or sum-GRW [2].

3 Assigning coordinates to descendant nodes in the GBG model

In the GBG model [5], nodes in the original layer are divided into r descendants with a probability p, increasing the population of nodes with branching rate b. The radius of the similarity subspace is rescaled as $R_{\ell-1} = bR_\ell$ to maintain a node density of one. The descendant nodes are assigned new coordiantes. Two conditions are imposed on the hidden degrees of descendant nodes: first, they must adhere to GR [6], meaning that their corresponding z values satisfy the transformations

$$z_{i_{\ell+1}} = \sum_{i_\ell \in i_{\ell+1}} z_{i_\ell}, \quad \theta_{i_{\ell+1}} = \frac{\sum_{i_\ell \in i_{\ell+1}} z_{i_\ell}\theta_{i_\ell}}{\sum_{i_\ell \in i_{\ell+1}} z_{i_\ell}}. \tag{1}$$

Second, the distribution of the descendants' hidden degrees $\rho(\kappa)$, or equivalently $\rho(z)$, must preserve that of the ancestor layer. Consequently, $\rho(z)$ must be a stable distribution [7]. By the generalized Central Limit Theorem [8], stable distributions are the only possible limit distributions for properly normalized and centered sums of *i.i.d.* random variables and encompass a rich family of models capable of accommodating fat tails and asymmetry. Concerning angular coordinates, descendants are positioned with slight angular offsets to the left and right of their ancestors, preventing overlaps between descendants of neighboring branching nodes. This transformation retains rotational invariance and the community structure (if present) encoded in the angular distribution of nodes.

4 Real space interpretation of the $k-$space LRG

The k-space LRG scheme given in the main text can be complemented with the following real space interpretation. Adopting the same notation, once

we have fixed the renormalization scale τ^*, one can consider the formation of $N_{\ell+1} = N_\ell - n(\tau^*)$ supernodes from the N_ℓ original micro-nodes, using the operator $K^{(\ell)}(\tau)$ through the following steps: (i) order the entries $|K^{(\ell)}_{i_\ell j_\ell}(\tau)|$ in descending order; (ii) merge micro-nodes into supernodes following this ordered list; (iii) stop when the desired number $N_{\ell+1}$ of clusters/supernodes is obtained. Clearly, this is only an approximated real-space representation of the k-space coarse-graining procedure. Also in statistical physics the relation between the real space coarse-graining with box cells *à la* Kadanoff and the k-space one, even if in principle possible for any local physical model through special functions, is quite complex and for practical purposes, intractable. Indeed, apart from trivial cases such as the $1D$-Ising model, tractable real-space formulations of the RG, such as the Niemeijer - Van Leeuwen cumulant technique and the Migdal-Kadanoff bond-moving decimation approach [9], give only approximated results with respect with the Wilson's k-space RG formulation coupled to field perturbation theories.

5 Laplacian operator and the Gaussian approximation of statistical dynamical models

In order to illustrate the relation between the network Laplacian operator and the Gaussian approximation of network theories of physical statistical models, we focus on the Ising model in a network with N vertices and M edges, whose dimensionless Hamiltonian can be written as:

$$\beta H[\boldsymbol{\sigma}, J, \mathbf{h}] = -\frac{J}{2}\sum_{i,j} A_{ij}\sigma_i\sigma_j - \sum_i h_i\sigma_i = \frac{J}{2}\sum_{i,j} L_{ij}\sigma_i\sigma_j - \sum_i h_i\sigma_i - JM$$
$$= \frac{J}{2}\sum_{i,j}\left(L_{ij} - \frac{2M}{N}\delta_{ij}\right)\sigma_i\sigma_j - \sum_i h_i\sigma_i\,,$$

where $J > 0$ is the coupling constant, $\beta > 0$ is the inverse temperature, the indices i, j run over the network vertices, A and L are the adjacency and Laplacian matrices of the network respectively, $\sigma_i = \pm 1$ is the spin variable related to the vertex i (with $\boldsymbol{\sigma}$ the whole spin configuration) and h_i is the external magnetic field acting on it (with $\mathbf{h}$ the whole field configuration). In the last two equalities we have used the fact that $\sigma_i^2 = 1$ in order to write the Hamiltonian in a convenient form. Note that in order to have the energy linearly growing with the number of network vertices N, we need to have

$J \sim N/M$. The partition function can be written as

$$Z(J, \mathbf{h}) = \sum_{\boldsymbol{\sigma}} e^{-H[\boldsymbol{\sigma}, J, \mathbf{h}]}$$

where the sum is extended to all possible spin configurations. We now note that, through the Hubbard-Stratonovich transformation [10], we can rewrite the model partition function $Z(J, \mathbf{h})$ in terms of a real scalar field $\boldsymbol{\psi}$ over nodes of the network, with vertex components ψ_i $(i = 1, ..., N)$, as:

$$\begin{aligned} Z(J, \mathbf{h}) \quad &= C \exp\left[\frac{1}{2J} \sum_{i,j} \left(B^{-1}\right)_{ij} h_i h_j\right] \iint_{-\infty}^{+\infty} \prod_i d\psi_i \qquad (2) \\ &\times \exp\left[\frac{J}{2} \sum_{i,j} B_{ij} \psi_i \psi_j + \sum_i \ln\cosh\left(J \sum_j B_{ij} \psi_j\right) + \sum_i h_i \psi_i\right], \end{aligned}$$

where C is a normalization constant and $B = \left(L - \frac{2M}{N} \mathbb{I}_N\right)$ is an $N \times N$ matrix constructed from L and the identity matrix $\mathbb{I}_N$. In order to obtain the Gaussian approximation of the above field theory, one has to develop the $\ln\cosh$ term to the second order in $\boldsymbol{\psi}$. The result is

$$Z(J, \boldsymbol{h}) \sim \int \mathcal{D}\boldsymbol{\psi}\, e^{-S_G[\boldsymbol{\psi}]}, \qquad (3)$$

where $\mathcal{D}\boldsymbol{\psi} = \prod_i d\psi_i$ and, adopting the bra-ket notation for the scalar product $\langle \psi | L | \psi \rangle = \sum_{i,j} L_{ij} \psi_i \psi_j$, we can write the Gaussian action $S_G[\boldsymbol{\psi}]$ as

$$\begin{aligned} S_G[\boldsymbol{\psi}] \quad &= \quad \frac{JM}{N}\left(1 - \frac{4MJ}{N}\right) \langle \psi | \psi \rangle + \frac{J}{2}\left(\frac{8MJ}{N} - 1\right) \langle \psi | L | \psi \rangle - J^2 \left\langle \psi | L^2 | \psi \right\rangle \\ &= \quad \sum_{\boldsymbol{\lambda}} \left[a(J) + b(J)\lambda - c(J)\lambda^2\right] \tilde{\psi}_\lambda^2, \qquad (4) \end{aligned}$$

where the last sum is over all the eigenvectors $\boldsymbol{\lambda}$ of L with eigenvalue λ, $a(J) = \frac{JM}{N}\left(1 - \frac{4MJ}{N}\right)$, $b(J) = \frac{J}{2}\left(\frac{8MJ}{N} - 1\right)$, $c(J) = J^2$ and $\tilde{\psi}_\lambda$ is the component $\langle \lambda | \psi \rangle$ of $\boldsymbol{\psi}$ along the eigenvector $\boldsymbol{\lambda}$. Note that: (i) this Gaussian action is diagonal in the basis of the eigenvectors of L which makes the integration of (3) exactly and easily computable; (ii) such a Gaussian approximation is valid only when the Gaussian distribution is normalizable and this is possible only if $1 - \frac{4MJ}{N} > 0$, i.e. unmagnetized / high temperature Gaussian phase; (iii) $J = \frac{N}{4M}$ is therefore the Gaussian critical point; (iv) $\left\langle \psi | L^2 | \psi \right\rangle$ at enough large scale (i.e. small eigenvalues region of L) is

subdominant with respect to $\langle\psi|L|\psi\rangle$ and can consequently be neglected sufficiently close to the critical point.

As shown in [11, 12], a large class of statistical physical models on regular lattices (e.g. contact processes, Kuramoto model of synchronizing oscillators) admit a field theory whose Gaussian approximation has a kernel which is similarly determined by the Laplacian operator (or the diffusion equation operator in case of dynamical statistical models). The extension of these models to regular networks are therefore characterized by an action for a continuous scalar field of the type

$$S[\boldsymbol{\psi}] = \sum_{\boldsymbol{\lambda}} (a + b\lambda)\tilde{\psi}_{\lambda}^{2} + F[\boldsymbol{\psi}]\,, \tag{5}$$

where $F[\boldsymbol{\psi}]$ is the higher-than-quadratic-order, non-Gaussian part of the action, which, in the hypothesis of renormalizability, is principle can be treated in the context of perturbation theory.

This shows the centrality of the Laplacian network operator in the characterization of the multiscale organization of a network and the interplay with the physical rules of the statical models embedded in it.

6 Higher order generalizations of LRG

Recently, generalizations of the LRG scheme to networks constructed from simplicial complexes and higher-order interactions have been also proposed [13, 14]. Using generalized notions of diffusion through higher-order Laplacian operators [15] one is able to model information flow between simplices of any order k via simplices of any other order m, so that cross-order Laplacians permits to probe the existence of characteristic scales in higher-order networks at each order. Specifically, it has been shown that is possible to extract a cross-order scale signature in simplicial complexes, showing that in most cases, scale-invariance is found only under the lens of specific orders, suggesting the existence of underlying order-specific processes [13]. It is also possible to introduce a simplex path integral and a simplex RG to represent trajectories based on a higher-order propagator, leading to a technique to average out short-range high-order interactions in dual k-space, while at the same time coarse-graining in real space to reduce the simplex structure encoding interactions among arbitrary sets of units [14].

7 Laplacian susceptibility, scale-invariance and spectral dimension

By its definition it is straightforward to show that the entropic susceptibility satisfies the following relationship [16, 17]

$$C(\tau) = -\tau^2 \frac{d\left\langle L^{(0)(\tau)}\right\rangle}{d\tau},$$

with the "quantum" mean of the Laplacian $L^{(0)}$ calculated through the probability measure induced by the density operator $\rho(\tau)$:

$$\left\langle L^{(0)}(\tau)\right\rangle \equiv \mathrm{Tr}[\rho(\tau)L^{(0)}] = -\frac{d\log Z(\tau)}{d\tau}.$$

Since $Z(\tau) = \sum_{i=1}^{N_0} e^{-\lambda_i^{(0)}\tau}$, one can also write

$$\left\langle L^{(0)}(\tau)\right\rangle \equiv \bar{\lambda}(\tau) = \frac{\int d\lambda\, \lambda\, \omega(\lambda) e^{-\lambda\tau}}{\int d\lambda\, \omega(\lambda) e^{-\lambda\tau}}, \tag{6}$$

where $\omega(\lambda) = \sum_{i=1}^{N_0} \delta(\lambda - \lambda_i^{(0)})/N_0$ is the spectral density of $L^{(0)}$ [18] which for large network sizes can be approximated as a continuous function at sufficiently small λ. It is now easy to show that $C(\tau)$ is independent of τ (a part from lower and upper cut-offs), meaning that the entropy rate of the Laplacian diffusion is scale independent, which can be used as a natural definition of topological scale invariance, *iif* $\omega(\lambda) \sim \lambda^\gamma$, i.e. the Laplacian spectral density is a power law, where γ is related to the spectral dimension d_s [19] through the relation $\gamma = d_s/2 - 1$, leading to $C(\tau) = d_s/2$.

A trivial example of such scale topological invariance is given by a regular lattice where d_s coincides with the simple spatial dimension d. Another simple but non trivial example, is given by random trees, with minimal branching ratio equal to 1 and finite variance of it, where $d_s = 4/3$. As shown in [16, 17], the Barabasi-Albert scale free network is scale invariant only in the case of new nodes entering with a single edge $m = 1$. In this case $d_s \simeq 2$. The scale invariance is lost for $m \geq 2$. Many other less trivial cases, both synthetic and real, can be found in [17].

From what above, we can conclude that $C(\tau)$ can be used as a detector of scale invariance of a real network, and in case its constant value provides a direct measure of the network spectral dimension.

8 Partition function of the multiscale model

In the multiscale renormalization approach, using the explicit form of the connection probability $p_{i_\ell j_\ell}(\mathbf{\Theta}_\ell)$ it is possible to rewrite the full graph probability $P\big(A^{(\ell)}|\mathbf{\Theta}_\ell\big)$ exactly as (dropping the dependence on the other parameters)

$$P(A^{(\ell)},\delta) = \frac{e^{-\mathcal{H}_{\text{eff}}^{(\ell)}\left(A^{(\ell)},\delta\right)}}{\mathcal{Z}(\delta)}, \tag{7}$$

where we have introduced the effective Hamiltonian

$$\mathcal{H}_{\text{eff}}^{(\ell)}(A^{(\ell)},\delta) \;\; = \;\; -\sum_{i_\ell=1}^{N_\ell}\sum_{j_\ell=1}^{i_\ell} a_{i_\ell j_\ell}^{(\ell)} \log\left[\frac{p_{i_\ell j_\ell}(\delta)}{1-p_{i_\ell j_\ell}(\delta)}\right] \tag{8}$$

and the partition function

$$Z(\delta) \equiv \sum_{A^{(\ell)}} e^{-\mathcal{H}_{\text{eff}}^{(\ell)}\left(A^{(\ell)},\delta\right)} = e^{\sum_{i_\ell=1}^{N_\ell}\sum_{j_\ell=1}^{N_\ell} x_{i_\ell}x_{j_\ell}f(d_{i_\ell j_\ell})/2}. \tag{9}$$

Note that, thanks to the renormalization rules for x_{i_ℓ} and $f(d_{i_\ell,j_\ell})$, the r.h.s. takes the same value irrespective of the level ℓ at which it is calculated [20], confirming that $Z(\delta)$ is invariant because we are at a fixed point of the renormalization flow.

References

[1] García-Pérez, G., Boguñá, M. & Serrano, M. Á. Multiscale unfolding of real networks by geometric renormalization. *Nat. Phys.* **14**, 583–589 (2018).

[2] Zheng, M., García-Pérez, G., Boguñá, M. & Serrano, M. Á. Geometric renormalization of weighted networks. *Communications Physics* **7**, 97 (2024).

[3] Allard, A., Serrano, M. Á., García-Pérez, G. & Boguñá, M. The geometric nature of weights in real complex networks. *Nat. Commun.* **8**, 14103 (2017).

[4] Chen, D., Su, H. & Zeng, Z. Geometric renormalization reveals the self-similarity of weighted networks. *IEEE Transactions on Computational Social Systems* 1–9 (2022).

[5] Zheng, M., García-Pérez, G., Boguñá, M. & Serrano, M. Á. Scaling up real networks by geometric branching growth. *Proceedings of the National Academy of Sciences* **118** (2021). URL `https://www.pnas.org/content/118/21/e2018994118`.

[6] García-Pérez, G., Boguñá, M. & Serrano, M. Á. Multiscale unfolding of real networks by geometric renormalization. *Nature Physics* **14**, 583–589 (2018).

[7] Nolan, J. P. *Stable Distributions-Models for Heavy Tailed Data* (Springer Nature, Boston, 2019).

[8] Lévy, P. Variables aléatoires. *Paris. Gauthier-Villars* (1937).

[9] Kardar, M. *Statitsical Physics of Fields* (Cambridge University Press, 2007).

[10] Amit, D. J. & Martin-Mayor, V. *Field theory, the renormalization group and critical phenomena* (World Scientific, 2005).

[11] Hinrichsen, H. Non-equilibrium critical phenomena and phase transitions into absorbing states. *Advances in Physics* **49**, 815–958 (2000).

[12] Dornic, I., Chaté, H. & Muñoz, M. A. Integration of Langevin equations with multiplicative noise and the viability of field theories for absorbing phase transitions. *Phys. Rev. Lett.* **94**, 100601 (2005).

[13] Nurisso, M. *et al.* Higher-order laplacian renormalization. *arXiv:2401.11298* (2024).

[14] Cheng, A., Xu, Y., Sun, P. & Tian, Y. A simplex path integral and a simplex renormalization group for high-order interactions. *Reports on Progress in Physics* **87**, 087601 (2024).

[15] Reitz, M. & Bianconi, G. The higher-order spectrum of simplicial complexes: a renormalization group approach. *Journal of Physics A: Mathematical and Theoretical* **53**, 295001 (2020).

[16] Villegas, P., Gili, T., Caldarelli, G. & Gabrielli, A. Laplacian renormalization group for heterogeneous networks. *Nature Physics* **19**, 445–450 (2023).

[17] Poggialini, A., Villegas, P., Muñoz, M. A. & Gabrielli, A. Networks with many structural scales: a renormalization group perspective. *Physical Review Letters* **134**, 057401 (2025).

[18] McGraw, P. N. & Menzinger, M. Laplacian spectra as a diagnostic tool for network structure and dynamics. *Phys. Rev. E* **77**, 031102 (2008).

[19] Burioni, R. & Cassi, D. Universal properties of spectral dimension. *Phys. Rev. Lett.* **76**, 1091–1093 (1996).

[20] Garuccio, E., Lalli, M. & Garlaschelli, D. Multiscale network renormalization: scale-invariance without geometry. *Physical Review Research* **5**, 043101 (2023).